as BAL.AN3. Although BAL.AN3 showed no proliferative response to BALB/c splenic DCs, BWF.AN3 showed a moderate proliferative response to BALB/c splenic DCs (Fig. 1*F*). These results suggest that the BWF1 T cell hyperreactivitiy enables BWF.AN3 to recognize small amounts of nucleosomal epitope presented on BALB/c splenic DCs, but these small amounts are ignored by BAL.AN3. As expected, BWF.AN3 strongly responded to BWF1 splenic DCs. Proliferative response of BWF.AN3 in the presence of BALB/c splenic DCs amounted to ~14–18% of that to BWF1 splenic DCs, indicating that the abnormal presentation of splenic DCs may contribute more to the autoreactive response than does T cell hyperreactivity.

To determine the general Ag recognition and reactivity of NZB/W F_1 mice, we examined the proliferation of T cells transduced with OVA-specific TCR (DO11.10). Fifty to 60% of the total $CD4^+$ T cells expressed the introduced DO11.10 TCR, as determined by the anti-clonotypic Ab KJ1-26. DO11.10-transduced BWF1 T cells cultured with DCs plus $OVA_{323-339}$ peptide exhibited stronger proliferation than BALB/c T cells, again suggesting that BWF1 T cells possess general hyperreactivity. In contrast, the OVA peptide-presentation (Fig. 1*G*) and the whole OVA presentation (data not shown) of NZB/W F_1 splenic DCs appeared to be quite similar to that of BALB/c splenic DCs. Thus, the hyperpresentation of DCs seems to be restricted to a certain Ag.

Nucleosome-specific T cells interacted with the autoantigen in the spleen

DCs in every type of lymphoid tissue may present nucleosomal epitopes, because nucleosomal Ags are available in every organ. To investigate this possibility, we fluorescently labeled either BWF.mock or BWF.AN3 T cells in vitro with CFSE and injected them into NZB/W F_1 mice. Two days after the transfer, T cells from the spleen and those from the peripheral lymph nodes (LNs) were harvested and analyzed. BWF.mock isolated from the spleen exhibited a convergent strong fluorescence peak, indicating that these cells had not proliferated extensively. In contrast, BWF.AN3 isolated from the spleen exhibited several weaker fluorescence peaks. Moreover, AN3 $CD4^+$ T cells underwent multiple divisions over a 5-day period of the experiment, and mock $CD4^+$ T cells underwent a very slight progression of cell division (Fig. 2*A*). These findings suggested that BWF.AN3 encountered the nucleosomal epitope in the spleen. It was of note that both CFSE-labeled BWF.mock and BWF.AN3 isolated from the peripheral LNs exhibited a strong convergent fluorescence peak, suggesting that BWF.AN3 encountered the nucleosomal epitope less frequently in the LNs.

A comparison of the stimulative capacity for BWF.AN3 also suggested that splenic DCs presented more nucleosomal epitope than DCs from the peripheral LNs (Fig. 2*B*). The average ratio of (BWsplDC − cpm)/(BWLNDC − cpm) was 2.79 ± 0.44 in three experiments ($p < 0.005$). These results showed that nucleosome-specific T cells are stimulated predominantly in the spleen.

Effect of CTLA4Ig transfer on the nucleosomal response

We next tried to generate nucleosome-specific regulatory cells by introducing an immunosuppressive molecule, CTLA4Ig, as the third gene in BWF.AN3 T cells. Long-term administration of CTLA4Ig to NZB/W F_1 mice has been shown to prevent disease onset for a period of months (29).

We constructed a pMX-CTLA4Ig-IRES-GFP vector (Fig. 1*A*). We then performed a triple gene transfer of the AN3$\alpha\beta$ and CTLA4Ig genes to investigate the effect on CTLA4Ig expression. The experimental groups consisted of $CD4^+$ T cells transduced with either AN3 + CTLA4Ig-IRES-GFP(CTLA4Ig), AN3 + IRES-GFP(IG), pMXW(mock) + CTLA4Ig, or mock + IG. The average expression efficiency from several different sets of infection was 45.2% for Vβ4 and 47.3% for GFP in $CD4^+$ cells (Fig. 3*A*). The average expression efficiency is expected to be 45% for the AN3α gene, and the average percentage of GFP^+AN3^+ cells expressing all three gene products in $CD4^+$ T cells was estimated to be ~10% (0.45 × 0.45 × 0.45). As shown in Fig. 3*B*, the CTLA4Ig secreted from T cells blocked the proliferation of the endogenous T cell population to the nucleosome to a moderate degree. The average ratio of (mock + CTLA4Ig with nuc − cpm)/(mock + IG with nuc − cpm) was 0.40 ± 0.07 in three experiments ($p < 0.005$). But the T cell stimulation mediated by AN3 TCR was not blocked by CTLA4Ig. The average ratio of (AN3 + IG − cpm)/(mock + IG − cpm) was 7.85 ± 1.07 and that of (AN3 + CTLA4Ig − cpm)/(mock + IG − cpm) was 7.18 ± 0.96 in three experiments. The AN3 + CTLA4Ig transduced cells showed the increase of CTLA4Ig secretion on T cell activation in the presence of DCs (Fig. 3*C*).

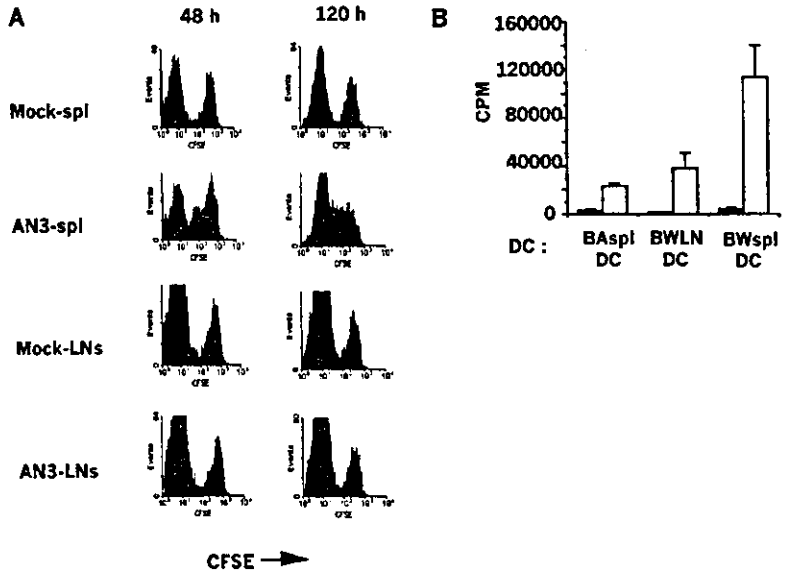

FIGURE 2. Nucleosome-specific T cells were stimulated more strongly in the spleen than in the LNs. *A*, CFSE-labeled BWF_1.mock T cells or BWF.AN3 T cells were transferred i.v. into 10-wk-old NZB/W F_1 mice. Two and 5 days later, splenocytes or peripheral LNs (cervical, inguinal, and mesenteric) from recipient mice were examined for $CFSE^+V\beta4^+$-gated cells. *B*, Proliferation of AN3- or mock-transduced T cells to $CD11c^+$ DCs from the spleen or LNs. $CD11c^+$ DCs from NZB/W F_1 spleens (BWsplDC), from NZB/W F_1 LNs (BWLNDC) and from BALB/c spleens (BAsplDC). Data shown are representative of three independent experiments with similar results.

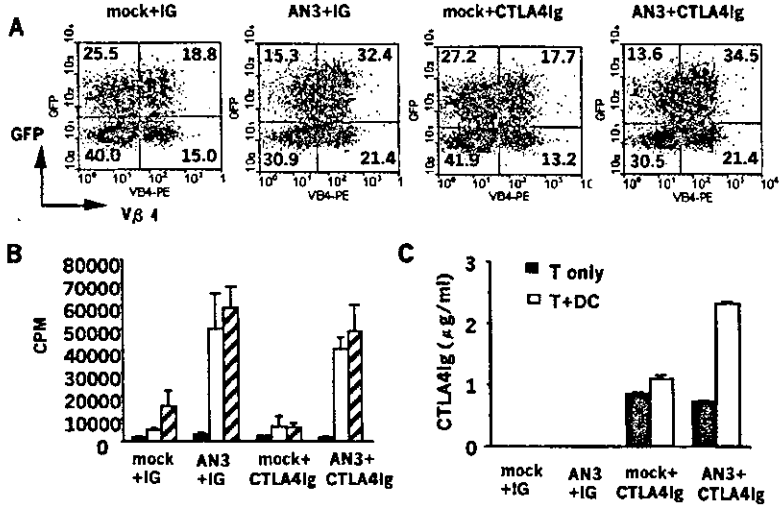

FIGURE 3. Effect of CTLA4Ig gene transfer on the T cell proliferation to nucleosomes. *A*, Expression analysis of GFP and Vβ4 in gene-transduced cells gated for CD4. The transduction efficiency was ~45% for a single gene in each group. *B*, Suppressive effect of CTLA4Ig transduction on T cell activation to nucleosomes. ■, T cells alone; □, T + DCs; ▨, T + DCs + nucleosome. *C*, CTLA4Ig production of T cells with or without DCs. Each culture supernatant was harvested after 24 h of culture. Data shown are representative of three independent experiments with similar results.

Nucleosome-specific regulatory cells suppressed autoimmune disease

We transferred cell suspensions containing 1×10^6 cells of $CD4^+$ T cells, calculatedly expressing either AN3 + CTLA4Ig, AN3 + IG, mock + CTLA4Ig, or mock + IG into 10-wk-old NZB/W F_1 mice.

The autoantibodies usually found in NZB/W F_1 mice were measured in the sera from the different groups. The elevations of anti-dsDNA and anti-histone Abs were suppressed in AN3 + CTLA4Ig-injected mice at 22 wk of age (Fig. 4*A*). AN3 + CTLA4Ig-injected mice showed the lowest average titer of anti-nucleosome Ab, but the titer in this group was not significantly different from those in the controls. This inefficient suppression may be due to the fact that autoimmunity to the nucleosome is the driving reaction and that this reaction is stronger than the subsequent response.

The mice were monitored biweekly for proteinuria. By week 22, control mice that had received PBS, mock + IG, AN3 + IG, or

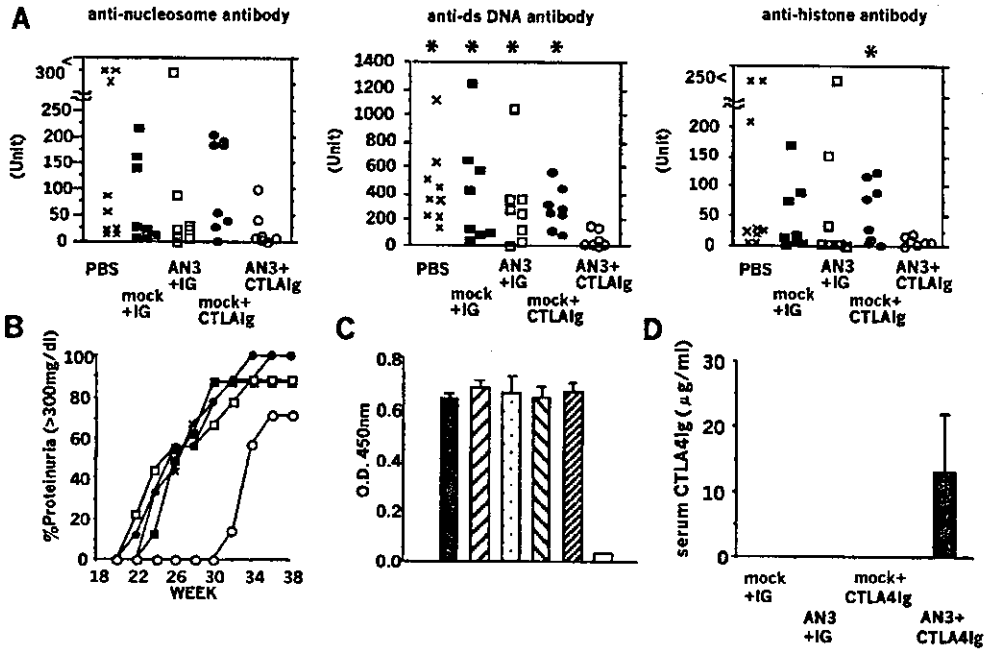

FIGURE 4. Effect of adoptively transferred engineered cells on disease progression. *A*, Suppression of autoantibody production. The elevation of serum anti-nucleosome, anti-dsDNA, and anti-histone Abs, measured by ELISA, was suppressed in AN3 + CTLA4Ig-injected mice at 22 wk. Statistically significant differences between AN3 + CTLA4Ig and control groups are denoted by asterisks ($p < 0.05$); $n = 7$ for AN3 + CTLA4Ig, and $n = 8$ for each control group. *B*, Cumulative percentage of mice in each group that developed severe proteinuria (>300 mg/dl). AN3 + CTLA4Ig showed suppressed progression of proteinuria compared with the control groups. x, PBS; ■, mock + IG; □, AN3 + IG; ●, mock + CTLA4Ig; ○, AN3 + CTLA4Ig. AN3 + CTLA4Ig vs the controls at 30 wk was significant ($p < 0.05$). *C*, A T cell-dependent humoral immune response to active immunization of OVA. Mice transferred with the engineered T cells at 10 wk of age were immunized with OVA in the footpad at 14 wk of age. Anti-OVA IgG Ab titer was measured at 17 wk of age. ■, PBS; ▨, mock + IG; ▩, AN3 + IG; ▧, mock + CTLA4Ig; ▨, AN3 + CTLA4Ig; □, no immunization. $n = 6$/group. *D*, Measurement of serum CTLA4Ig protein in the experimental groups with ELISA. Only AN3 + CTLA4Ig-transferred mice showed detectable, but low concentration of CTLA4Ig protein.

mock + CTLA4Ig started developing severe nephritis, as diagnosed by persistent proteinuria of >300 mg/dl. By 30 wk of age, 89% of the PBS control group, 88% of the mock + IG group, 63% of the AN3 + IG group, and 75% of the mock + CTLA4Ig group of mice had developed severe proteinuria, whereas none of the AN3 + CTLA4Ig mice showed excess proteinuria (Fig. 4*B*). However, the AN3 + CTLA4Ig-transferred mice started to develop severe proteinuria at 32 wk of age. Splenomegaly and an increase in the CD4:CD8 ratio, usually observed in aged NZB/W F_1 mice, were suppressed in AN3 + CTLA4Ig-injected mice (data not shown).

The kidneys from the controls and AN3 + CTLA4Ig-injected mice were examined at 30 wk of age (Fig. 5, *A–F*). Control mice had severe glomerulonephritis with mesangial proliferation and thickening of the capillary walls with marked deposition of IgG and complement. AN3 + CTLA4Ig-injected mice had mild glomerular lesions and deposition of IgG and complement was only restricted to the mesangial area. Although mock + CTLA4Ig-transferred mice showed formation of a number of large follicles with T cell invasion in the spleen, AN3 + CTLA4Ig-transferred mice showed only a limited number of small follicles (Fig. 5, *G* and *H*).

AN3 + CTLA4Ig-treated mice exhibited the normal humoral immune response upon active immunization

We next examined the T cell-dependent humoral immune response to active immunization of OVA. Mice transferred with the engineered T cells at 10 wk of age were immunized with OVA (100 μg) with CFA at 14 wk of age and boosted with OVA with IFA at 16 wk of age. The level of anti-OVA IgG Ab titer from 17-wk-old mice treated with AN3 + CTLA4Ig was not significantly different from those of the control mice (Fig. 4*C*). AN3 + CTLA4Ig transferred mice, but not other experimental groups, had low but detectable levels of serum CTLA4Ig (13.4 ± 10.1 μg/ml) (Fig. 4*D*), findings consistent with in vitro data shown in Fig. 3*C*. These results suggest that the engineered regulatory cells are sufficient to suppress autoimmune disease. However, they are not enough to induce general immunosuppression, because of the low serum level of CTLA4Ig in AN3 + CTLA4Ig-transferred mice.

Discussion

In this study, we demonstrated T cell hyperresponsiveness and the possibility of nucleosomal hyperpresentation of splenic DCs in NZB/W F_1 mice. In addition to the involvement of T cell hyperresponsiveness in Ab-mediated autoimmune disease (30), our results strongly suggest that the autoantigen hyperpresentation of DCs could contribute to the initiation and propagation of the response to the autoantigen, thereby resulting in florid autoimmune disease. This observation is consistent with those from previous reports indicating that mice with T cell hyperresponsiveness develop only a mild form of lupus-like symptoms (31, 32). Since hyperpresentation was not observed in the case of an exogenous Ag, OVA (peptides and whole protein), it is possible that the autoantigen hyperpresentation of splenic DCs was not due to the general hyperpresentation, e.g., excessive costimulatory signals, but rather to some Ag-restricted phenomenon. These features may be nucleosome specific, as reported in a previous study demonstrating that lupus-prone B6.NZMc1 mice showed nucleosome reactivity of T cells without generalized immunological deficits of B cells and T cells (33).

Although disease-related increases in the number of splenic DCs and chemokine production by myeloid DCs have been reported (34), these abnormalities have been observed in aged lupus-prone mice. Our finding of autoantigen hyperpresentation in the splenic DCs of young mice (10 wk) suggests the significance of the autoantigen hyperpresentation of splenic DCs in the pathogenesis of lupus.

Autoreactive response of nucleosome-specific T cells was much more prominent in the spleen than in the LNs. Although the mixed I-A haplotype of Aβz/Aαd molecules in NZB/W F_1 mice (35) may be associated with autoreactive response of AN3 infectant, the absence of the autoreactivity to B cells and DCs from peripheral LNs strongly suggests the requirement of an autoantigen for the autoreactivity. Differences between the splenic DCs and DCs from other peripheral lymphoid organs have been reported, including differences in the expression of chemokines (36) and chemokine receptors (37). Otherwise, localization of tissue-specific autoantigen among secondary lymphoid organs may be one explanation. For example, although DCs in the gastric LNs are known to exhibit constitutive presentation of gastric parietal cell-specific H^+/K^+-ATPase, peripheral or mesenteric DCs do not (38). Thus, the spleen could be one of the main sources of nucleosomes. Increased frequency of splenic apoptosis in SNF1 lupus mice has also been reported (23). Moreover, an insufficient complement system may allow apoptotic waste material to accumulate in the spleen (i.e., the "waste disposal" hypothesis) (39).

In our study, the therapeutic effect with minimal systemic immunosuppression was archived by the use of nucleosome-specific T cells secreting CTLA4Ig. Although elevation of CTLA4Ig protein was detected in the serum of AN3 + CTLA4Ig mice, the

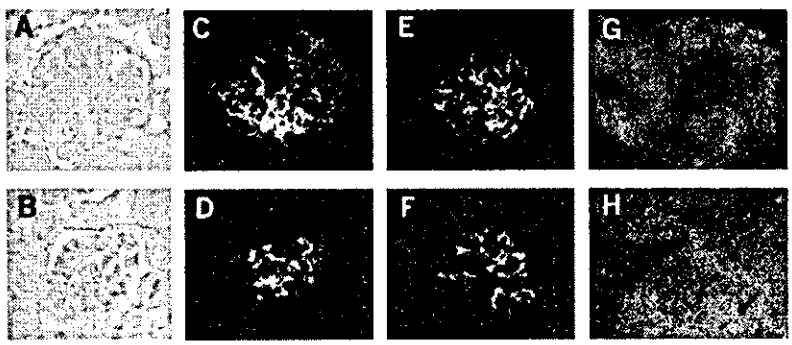

FIGURE 5. Histological examination from the AN3 + CTLA4Ig-treated mice compared with control mice. Sections of kidney from mock + IG-injected mice (*A*, *C*, and *E*) and AN3 + CTLA4Ig-injected mice (*B*, *D*, and *F*) subjected to staining with periodic-acid-Schiff solution (*A* and *B*) or to immunofluorescence staining with anti-IgG (*C* and *D*) or anti-C3 (*E* and *F*). Immunofluorescence staining of sections from the spleen, from mock + CTLA4Ig-injected mice (*G*), and from AN3 + CTLA4Ig-injected mice (*H*) with Abs to B220 (green), CD4 and CD8 (red), and with peanut agglutinin (blue). A section from one representative mouse from the indicated group is shown.

average concentration of CTLA4Ig in AN3 + CTLA4Ig mice is less than one-tenth of the level of previous systemic CTLA4Ig treatment with 5×10^8 PFU of adenovirus (27). Although the systemic adenoviral-CTLA4Ig (5×10^8 PFU) treatment exhibited a therapeutic effect equivalent to that of our experiment, the systemic treatment was accompanied with generalized immunosuppression. Since autoantigen-specific CTLA4Ig-secreting T cells showed normal Ab production on active immunization, this treatment may be superior to systemic CTLA4Ig administration. However, a systemic effect of a very low level of CTLA4Ig cannot be excluded and should be investigated further.

It is not surprising that 10^6 AN3 + mock cells did not aggravate the disease, since as many as 4×10^7 original L3A clone cells were needed to accelerate lupus nephritis in young lupus-prone mice (40). Thus, a relatively small amount of Ag-specific and potentially pathogenic T cells could be used for the immunotherapy. Foxp3, a member of the transcription factor family, has been identified as a key molecule for the development of $CD4^+CD25^+$ regulatory T cells (41). Retroviral transfer of Foxp3 confers regulatory function on $CD4^+CD25^-$ T cells. The introduction of such regulatory molecules with TCR could possibly generate Ag-specific regulatory T cells.

In a preliminary analysis of the persistence of the transferred genes in the spleen and LNs from 30-wk-old mice with RT-PCR, expression of AN3α gene was detected in the spleens from two of two AN3 + IG^- and AN3 + $CTLA4Ig^-$-injected mice (data not shown). These results may suggest the persistence of introduced genes at 20 wk after the transfer in the spleen.

Although several models of adoptive cell gene therapy have been reported using T cell hybridomas or lines (42, 43), our method has the advantage of using autologous lymphocytes for gene recipients. However, TCR-transduced recipient T cells could gain heterodimeric TCR consisting of endogenous and exogenous chains. If such an unexpected TCR recognizes a certain unrelated self-derived molecule, the transduced T cells may be harmful. We did not observe evident autoreactivity in single AN3α or AN3β genes transferred into $CD4^+$ T cells (data not shown), and the renal disease of AN3 TCR-transferred mice was not accelerated (Fig. 5*B*). There was a recent report of tumor rejection mediated by retrovirally reconstituted Ag-specific T cells without any significant autoimmune pathology (44, 45). However, the possibility of developing autoimmunity should be carefully investigated further in application of TCR gene transfer.

In the present study, the efficacy of triple gene transfer in peripheral T cells was demonstrated for the first time. Although several improvements of the present method are still necessary, these findings suggest that the direct engineering of Ag-specific functional cells with multiple gene transfer is a powerful technique for the development of future Ag-specific therapies.

Acknowledgments

We are grateful to Kazumi Abe and Shiho Ohta for their excellent technical assistance.

References

1. Zitvogel, L., J. I. Mayordomo, T. Tjandrawan, A. B. DeLeo, M. R. Clarke, M. T. Lotze, and W. J. Storkus. 1996. Therapy of murine tumors with tumor peptide-pulsed dendritic cells: dependence on T cells, B7 costimulation, and T helper cell 1-associated cytokines. *J. Exp. Med. 183:87.*
2. Nestle, F. O., S. Alijagic, M. Gilliet, Y. Sun, S. Grabbe, R. Dummer, G. Burg, and D. Schadendorf. 1998. Vaccination of melanoma patients with peptide- or tumor lysate-pulsed dendritic cells. *Nat. Med. 4:328.*
3. Steinberg, A. D., M. F. Gourley, D. M. Klinman, G. C. Tsokos, D. E. Scott, and A. M. Krieg. 1991. NIH conference: systemic lupus erythematosus. *Ann. Intern. Med. 115:548.*
4. Lambert, P. H., and F. J. Dixon. 1968. Pathogenesis of the glomerulonephritis of NZB/W mice. *J. Exp. Med. 127:507.*
5. Dixon, F. J., M. B. Oldstone, and G. Tonietti. 1971. Pathogenesis of immune complex glomerulonephritis of New Zealand mice. *J. Exp. Med. 134(Suppl.):65s.*
6. Winfield, J. B., I. Faiferman, and D. Koffler. 1977. Avidity of anti-DNA antibodies in serum and IgG glomerular eluates from patients with systemic lupus erythematosus: association of high avidity antinative DNA antibody with glomerulonephritis. *J. Clin. Invest. 59:90.*
7. Mohan, C., S. Adams, V. Stanik, and S. K. Datta. 1993. Nucleosome: a major immunogen for pathogenic autoantibody-inducing T cells of lupus. *J. Exp. Med. 177:1367.*
8. Kaliyaperumal, A., C. Mohan, W. Wu, and S. K. Datta. 1996. Nucleosomal peptide epitopes for nephritis-inducing T helper cells of murine lupus. *J. Exp. Med. 183:2459.*
9. Lu, L., A. Kaliyaperumal, D. T. Boumpas, and S. K. Datta. 1999. Major peptide autoepitopes for nucleosome-specific T cells of human lupus. *J. Clin. Invest. 104:345.*
10. Burlingame, R. W., R. L. Rubin, R. S. Balderas, and A. N. Theofilopoulos. 1993. Genesis and evolution of antichromatin autoantibodies in murine lupus implicates T-dependent immunization with self antigen. *J. Clin. Invest. 91:1687.*
11. Burlingame, R. W., M. L. Boey, G. Starkebaum, and R. L. Rubin. 1994. The central role of chromatin in autoimmune responses to histones and DNA in systemic lupus erythematosus. *J. Clin. Invest. 94:184.*
12. Amoura, Z., S. Koutouzov, H. Chabre, P. Cacoub, I. Amoura, L. Musset, J. F. Bach, and J. C. Piette. 2000. Presence of antinucleosome autoantibodies in a restricted set of connective tissue diseases: antinucleosome antibodies of the IgG3 subclass are markers of renal pathogenicity in systemic lupus erythematosus. *Arthritis Rheum. 43:76.*
13. Bruns, A., S. Blass, G. Hausdorf, G. R. Burmester, and F. Hiepe. 2000. Nucleosomes are major T and B cell autoantigens in systemic lupus erythematosus. *Arthritis Rheum. 43:2307.*
14. Desai-Mehta, A., L. Lu, R. Ramsey-Goldman, and S. K. Datta. 1996. Hyperexpression of CD40 ligand by B and T cells in human lupus and its role in pathogenic autoantibody production. *J. Clin. Invest. 97:2063.*
15. Liossis, S. N., B. Kovacs, G. Dennis, G. M. Kammer, and G. C. Tsokos. 1996. B cells from patients with systemic lupus erythematosus display abnormal antigen receptor-mediated early signal transduction events. *J. Clin. Invest. 98:2549.*
16. Wofsy, D., and W. E. Seaman. 1985. Successful treatment of autoimmunity in NZB/NZW F_1 mice with monoclonal antibody to L3T4. *J. Exp. Med. 161:378.*
17. Donello, J. E., J. E. Loeb, and T. J. Hope. 1998. Woodchuck hepatitis virus contains a tripartite posttranscriptional regulatory element. *J. Virol. 72:5085.*
18. Zufferey, R., J. E. Donello, D. Trono, and T. J. Hope. 1999. Woodchuck hepatitis virus posttranscriptional regulatory element enhances expression of transgenes delivered by retroviral vectors. *J. Virol. 73:2886.*
19. Kitamura, T., M. Onishi, S. Kinoshita, A. Shibuya, A. Miyajima, and G. P. Nolan. 1995. Efficient screening of retroviral cDNA expression libraries. *Proc. Natl. Acad. Sci. USA 92:9146.*
20. Wallace, P. M., J. S. Johnson, J. F. MacMaster, K. A. Kennedy, P. Gladstone, and P. S. Linsley. 1994. CTLA4Ig treatment ameliorates the lethality of murine graft-versus-host disease across major histocompatibility complex barriers. *Transplantation 58:602.*
21. Kawashima, T., K. Hirose, T. Satoh, A. Kaneko, Y. Ikeda, Y. Kajiro, T. Nosaka, and T. Kitamura. 2000. MgcRacGAP is involved in the control of growth and differentiation of hematopoietic cells. *Blood 96:2116.*
22. Fujio, K., Y. Misaki, K. Setoguchi, S. Morita, K. Kawahata, I. Kato, T. Nosaka, K. Yamamoto, and T. Kitamura. 2000. Functional reconstitution of class II MHC-restricted T cell immunity mediated by retroviral transfer of the $\alpha\beta$ TCR complex. *J. Immunol. 165:528.*
23. Morita, S., T. Kojima, and T. Kitamura. 2000. Plat-E: an efficient and stable system for transient packaging of retroviruses. *Gene Ther. 7:1063.*
24. Kalled, S. L., A. H. Cutler, and L. C. Burkly. 2001. Apoptosis and altered dendritic cell homeostasis in lupus nephritis are limited by anti-CD154 treatment. *J. Immunol. 167:1740.*
25. Akbari, O., R. H. DeKruyff, and D. T. Umetsu. 2001. Pulmonary dendritic cells producing IL-10 mediate tolerance induced by respiratory exposure to antigen. *Nat. Immunol. 2:725.*
26. Bates, D. L., P. J. Butler, E. C. Pearson, and J. O. Thomas. 1981. Stability of the higher-order structure of chicken-erythrocyte chromatin in solution. *Eur. J. Biochem.119:469*
27. Mihara, M., I. Tan, Y. Chuzhin, B. Reddy, L. Budhai, A. Holzer, Y. Gu, and A. Davidson. 2000. CTLA4Ig inhibits T cell-dependent B-cell maturation in murine systemic lupus erythematosus. *J. Clin. Invest. 106:91.*
28. Shi, Y., A. Kaliyaperumal, L. Lu, S. Southwood, A. Sette, M. A. Michaels, and S. K. Datta. 1998. Promiscuous presentation and recognition of nucleosomal autoepitopes in lupus: role of autoimmune T cell receptor α chain. *J. Exp. Med. 187:367.*
29. Finck, B. K., P. S. Linsley, and D. Wofsy. 1994. Treatment of murine lupus with CTLA4Ig. *Science 265:1225.*
30. Vratsanos, G. S., S. Jung, Y. M. Park, and J. Craft. 2001. $CD4^+$ T cells from lupus-prone mice are hyperresponsive to T cell receptor engagement with low and high affinity peptide antigens: a model to explain spontaneous T cell activation in lupus. *J. Exp. Med. 193:329.*
31. Murga, M., O. Fernandez-Capetillo, S. J. Field, B. Moreno, L. R. Borlado, Y. Fujiwara, D. Balomenos, A. Vicario, A. C. Carrera, S. H. Orkin, M. E. Greenberg, and A. M. Zubiaga. 2001. Mutation of E2F2 in mice causes enhanced T lymphocyte proliferation, leading to the development of autoimmunity. *Immunity 15:959.*

32. Mohan, C., Y. Yu, L. Morel, P. Yang, and E. K. Wakeland. 1999. Genetic dissection of Sle pathogenesis: Sle3 on murine chromosome 7 impacts T cell activation, differentiation, and cell death. *J. Immunol. 162:6492.*
33. Mohan, C., E. Alas, L. Morel, P. Yang, and E. K. Wakeland. 1998. Genetic dissection of SLE pathogenesis: Sle1 on murine chromosome 1 leads to a selective loss of tolerance to H2A/H2B/DNA subnucleosomes. *J. Clin. Invest. 101: 1362.*
34. Ishikawa, S., T. Sato, M. Abe, S. Nagai, N. Onai, H. Yoneyama, Y. Zhang, T. Suzuki, S. Hashimoto, T. Shirai, M. Lipp, and K. Matsushima. 2001. Aberrant high expression of B lymphocyte chemokine (BLC/CXCL13) by $C11b^+CD11c^+$ dendritic cells in murine lupus and preferential chemotaxis of B1 cells towards BLC. *J. Exp. Med. 193:1393.*
35. Gotoh, Y., H. Takashima, K. Noguchi, H. Nishimura, M. Tokushima, T. Shirai, and M. Kimoto. 1993. Mixed haplotype Abz/Aad class II molecule in (NZB × NZW)F_1 mice detected by T cell clones. *J. Immunol. 150: 4777.*
36. Yoneyama, H., S. Narumi, Y. Zhang, M. Murai, M. Baggiolini, A. Lanzavecchia, T. Ichida, H. Asakura, and K. Matsushima. 2002. Pivotal role of dendritic cell-derived CXCL10 in the retention of T helper cell 1 lymphocytes in secondary lymph nodes. *J. Exp. Med. 195:1257.*
37. Iwasaki, A., and B. L. Kelsall. 2000. Localization of distinct Peyer's patch dendritic cell subsets and their recruitment by chemokines macrophage inflammatory protein (MIP)-3α, MIP-3β, and secondary lymphoid organ chemokine. *J. Exp. Med. 191:1381.*
38. Scheinecker, C., R. McHugh, E. M. Shevach, and R. N. Germain. 2002. Constitutive presentation of a natural tissue autoantigen exclusively by dendritic cells in the draining lymph node. *J. Exp. Med. 196:1079.*
39. Walport, M. J. 2001. Complement. *N. Engl. J. Med. 344:1140.*
40. Adams, S., P. Leblanc, and S. K. Datta. 1991. Junctional region sequences of T-cell receptor β-chain genes expressed by pathogenic anti-DNA autoantibody-inducing helper T cells from lupus mice: possible selection by cationic autoantigens. *Proc. Natl. Acad. Sci. USA 88:11271.*
41. Hori, S., T. Nomura, and S. Sakaguchi. 2003. Control of regulatory T cell development by the transcription factor Foxp3. *Science 299:1057.*
42. Setoguchi, K., Y. Misaki, Y. Araki, K. Fujio, K. Kawahata, T. Kitamura, and K. Yamamoto. 2000. Antigen-specific T cells transduced with IL-10 ameliorate experimentally induced arthritis without impairing the systemic immune response to the antigen. *J. Immunol. 165:5980.*
43. Nakajima, A., C. M. Seroogy, M. R. Sandora, I. H. Tarner, G. L. Costa, C. Taylor-Edwards, M. H. Bachmann, C. H. Contag, and C. G. Fathman. 2001. Antigen-specific T cell-mediated gene therapy in collagen-induced arthritis. *J. Clin. Invest. 107:1293.*
44. Kessels, H. W., M. C. Wolkers, M. D. van den Boom, M. A. van der Valk, and T. N. Schumacher. 2001. Immunotherapy through TCR gene transfer. *Nat. Immunol. 2:957.*
45. Schumacher, T. N. 2002. T-cell-receptor gene therapy. *Nat. Rev. Immunol. 2:512.*

nature
genetics

© 2003 Nature Publishing Group http://www.nature.com/naturegenetics

Functional haplotypes of *PADI4*, encoding citrullinating enzyme peptidylarginine deiminase 4, are associated with rheumatoid arthritis

Akari Suzuki[1], Ryo Yamada[1], Xiaotian Chang[1], Shinya Tokuhiro[1,2], Tetsuji Sawada[3], Masakatsu Suzuki[2], Miyuki Nagasaki[2], Makiko Nakayama-Hamada[2], Reimi Kawaida[2], Mitsuru Ono[2], Masahiko Ohtsuki[2], Hidehiko Furukawa[2], Shinichi Yoshino[4], Masao Yukioka[5], Shigeto Tohma[6], Tsukasa Matsubara[7], Shigeyuki Wakitani[8], Ryota Teshima[9], Yuichi Nishioka[10], Akihiro Sekine[11], Aritoshi Iida[11], Atsushi Takahashi[12], Tatsuhiko Tsunoda[12], Yusuke Nakamura[11,13] & Kazuhiko Yamamoto[1,3]

Individuals with rheumatoid arthritis frequently have autoantibodies to citrullinated peptides, suggesting the involvement of the peptidylarginine deiminases citrullinating enzymes (encoded by *PADI* genes) in rheumatoid arthritis. Previous linkage studies have shown that a susceptibility locus for rheumatoid arthritis includes four *PADI* genes but did not establish which *PADI* gene confers susceptibility to rheumatoid arthritis. We used a case-control linkage disequilibrium study to show that *PADI* type 4 is a susceptibility locus for rheumatoid arthritis ($P = 0.000008$). *PADI4* was expressed in hematological and rheumatoid arthritis synovial tissues. We also identified a haplotype of *PADI4* associated with susceptibility to rheumatoid arthritis that affected stability of transcripts and was associated with levels of antibody to citrullinated peptide in sera from individuals with rheumatoid arthritis. Our results imply that the *PADI4* haplotype associated with susceptibility to rheumatoid arthritis increases production of citrullinated peptides acting as autoantigens, resulting in heightened risk of developing the disease.

Rheumatoid arthritis is one of the most common human systemic autoimmune diseases. It is characterized by inflammation of synovial tissues and the formation of rheumatoid pannus, which is capable of eroding adjacent cartilage and bone and causing subsequent joint destruction. Previous studies have indicated that risk of the disease in siblings of affected individuals (λ_{sib}) is 2–17 times higher, suggesting the importance of genetic factors in rheumatoid arthritis[1]. Multiple genes are believed to contribute to rheumatoid arthritis susceptibility, but the only locus that has been conclusively associated with the condition is the *HLA-DRB* locus, which accounts for about one third of the genetic component[2–4]. Recently, four sibling-pair linkage studies from Europe, North America and Japan were published[5–8]. Although no common loci apart from the *HLA* region were suggested by all the studies, some were suggested by multiple studies. Chromosome 1p36 represents one such locus. Cornelis *et al.*[5] reported an association between rheumatoid arthritis and *D1S228* that identified nucleotides 363,575–363,702 on NT_004873.12 in a study using 114 sibling pairs ($P = 0.0065$). Shiozawa *et al.*[8] obtained a single-point lod score of 3.58 at *D1S214* that identified nucleotides 1,089,077–108,972 on NT_028054.9 and also observed lod scores of 3.77 as a single-point analysis and 6.13 as a multi-point analysis at *D1S253* that identified a region 1.5 cM telomeric from *D1S214* (located in GB4 map by the International RH Mapping Consortium but not annotated in the Reference Sequence of genomic DNA by NCBI), using 41 families. *D1S228* and *D1S214* are located 6.7 Mb apart according to the Reference Sequence build 33 from the National Center for Biotechnology Information.

The gene region located 3.1 Mb and 9.8 Mb centromeric from *D1S228* and *D1S214*, respectively, contains clusters of enzymes that are functionally associated with the production of rheumatoid arthritis–specific autoantibodies. These enzymes are the peptidylarginine deiminases (PADIs), which posttranslationally convert arginine residues to citrulline. Citrullinated epitopes involved in a peptidic link are the most specific targets of rheumatoid arthritis–specific autoantibodies. Citrullination is related to two rheumatoid arthritis–specific autoantibody systems: those directed against perinuclear factor/keratin and against Sa[9,10]. Assays of antibodies to citrullinated peptide can

[1]Laboratory for Rheumatic Diseases, SNP Research Center, The Institute of Physical and Chemical Research (RIKEN), 1-7-22, Suehirocho, Tsurumi-ku, Yokohama City, Kanagawa 230-0045, Japan. [2]Sankyo, Tokyo, Japan. [3]Department of Allergy and Rheumatology, Graduate School of Medicine, the University of Tokyo, Tokyo, Japan. [4]Department of Joint Disease and Rheumatism, Nippon Medical School, Tokyo, Japan. [5]Yukioka Hospital, Osaka, Japan. [6]National Sagamihara Hospital, Kanagawa, Japan. [7]Matsubara Mayflower Hospital, Hyogo, Japan. [8]Osaka Minami National Hospital, Osaka, Japan. [9]Department of Orthopedic Surgery, Tottori University, Tottori, Japan. [10]Yamanashi Prefectural Central Hospital, Yamanashi, Japan. [11]Laboratory for Genotyping and [12]Laboratory for Medical Informatics, SNP Research Center, The Institute of Physical and Chemical Research (RIKEN), Kanagawa, Japan. [13]Laboratory of Molecular Medicine, Human Genome Center, Institute of Medical Science, University of Tokyo, Tokyo, Japan. Correspondence should be addressed to R.Y. (ryamada@src.riken.go.jp).

be used as valuable diagnostic tools[11,12]. The clinical importance of measuring antibodies to citrullinated peptide and the specificity of autoantibodies suggests a specific role of citrullination and PADIs in the pathophysiology of rheumatoid arthritis. In addition, the appearance of antibodies to citrullinated peptide in sera from affected individuals in the very early phase of disease manifestation implies that citrullination is involved in the triggering phase or the acute phase of the disease[13]. The presence of citrullinated peptides in rheumatoid arthritis synovial tissue has also been reported, suggesting the involvement of PADIs in the pathomechanisms of rheumatoid arthritis[14–16].

We carried out a case-control association study using single-nucleotide polymorphisms (SNPs) discovered by the Japanese Millennium Genome Project in the 1p36 region containing the genes *PADI1*, *PADI2*, *PADI3* and *PADI4*. This study identified a haplotype associated with susceptibility to rheumatoid arthritis in *PADI4* but not in neighboring *PADI* genes. We confirmed that *PADI4* was expressed in hematological cells by northern-blot hybridization and in synovial tissue of individuals with rheumatoid arthritis by *in situ* RT–PCR and immunohistochemistry. Moreover, the susceptibility haplotype of *PADI4* was related to levels of antibody to citrullinated filaggrin in sera of individuals with rheumatoid arthritis. We also identified a difference in mRNA stability between non-susceptibility and susceptibility variants of *PADI4*.

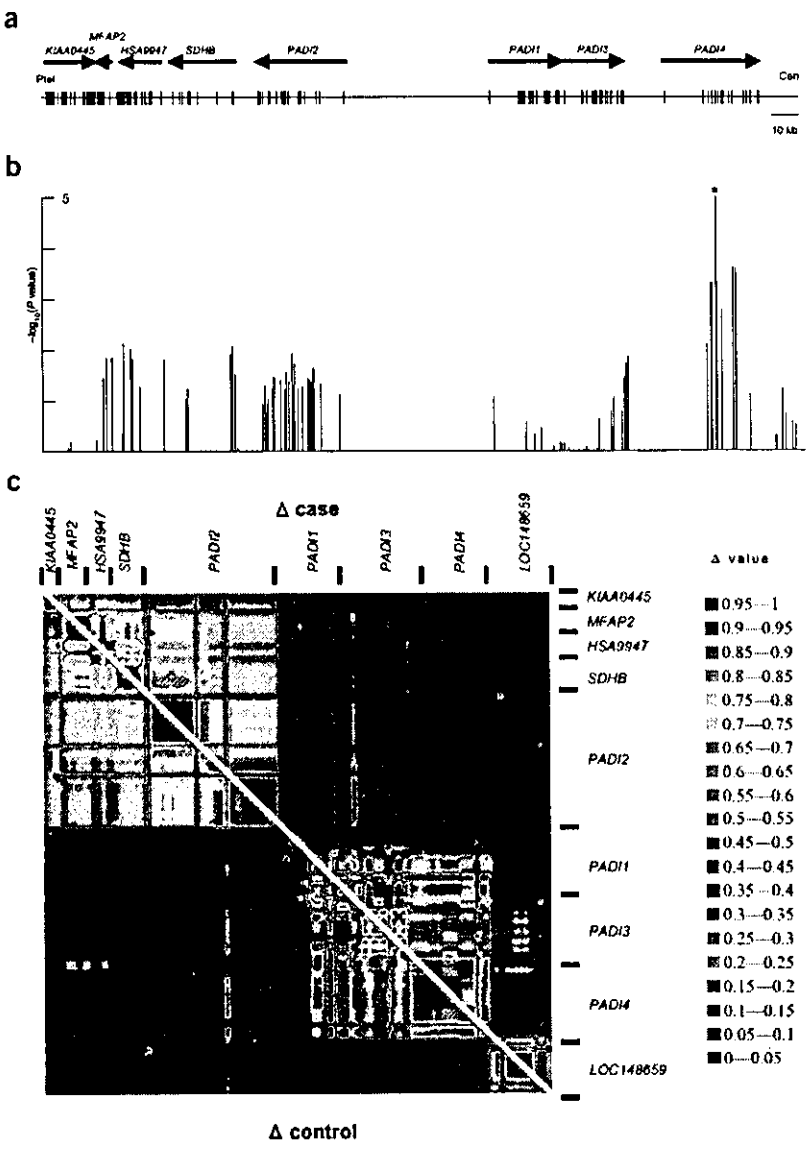

Figure 1 Gene content of NT_034367.1 in chromosome 1p36, case-control association and linkage disequilibrium. (**a**) Genomic structure of genes in this region. Ptel, p telomere; Cen, centromere. (**b**) Case-control association plots ($-\log_{10}(P \text{ value})$) versus location in this region. Asterisk indicates the SNP showing the strongest association in this region. (**c**) Pairwise linkage disequilibrium between SNPs, as measured by Δ in the case and control populations in this region: upper right triangle, case population; lower left triangle, control population.

RESULTS

Case-control study using SNPs in NT_034376.1

To identify genes associated with susceptibility to rheumatoid arthritis, we focused on the region NT_034376.1 on chromosome 1p36, in which we had previously identified the SNP strongly associated with rheumatoid arthritis. This region contains eight genes (including four *PADI* genes) that could be associated with rheumatoid arthritis according to the data regarding antibodies to citrullinated peptides. We refined the location of the rheumatoid arthritis susceptibility locus in a case-control study using 119 SNPs distributed in genes across contig NT_034376.1 (**Fig. 1a,b** and **Supplementary Table 1** online). The total length we evaluated was 445,670 bp, and SNPs were located every 3.7 kb on average. We predominantly used the Invader assay, which can efficiently detect genotypes of SNPs[17,18], and analyzed samples from a total of 830 affected individuals and 736 unaffected controls. Overall success rates of typing assays for cases and controls were 96% and 95%, respectively. A SNP in *PADI4*, padi4_94 (28017T in intron 3, susceptible; →C, non-susceptible), had the most significant association with rheumatoid arthritis ($\chi^2 = 19.856$, $P = 0.000008$ comparing allele 1 versus allele 2; odds ratio (OR) = 1.97, 95% confidence interval (c.i.) = 1.44–2.69 comparing susceptible homozygotes versus non-susceptible homozygotes; **Table 1** and **Fig. 1b**). When Bonferroni's correction was applied to the result we obtained $P = 0.00095$, and the Monte Carlo Permutation test gave $P = 0.00003$ with 1×10^6 replications[19]. Both of these results were statistically significant.

We then sequenced all exons of *PADI4*, including the 5′ and 3′ untranslated regions, from 48 individuals with rheumatoid arthritis to identify SNPs. We identified four new SNPs and genotyped them in the exons: padi4_89 (163G→A in exon 2), padi4_90 (245T→C in exon 2), padi4_92 (335G→C in

© 2003 Nature Publishing Group http://www.nature.com/naturegenetics

Table 1 Summary of association between cases and controls in *PADI4*

	Genotype of case				Genotype of control				Allele 1 versus allele 2		Genotype 11 versus genotype 22
SNP ID	11	12	22	Sum	11	12	22	Sum	χ^2	*P* value	OR (95% c.i.)
padi4_92	166	416	241	823	102	307	246	655	12.36	0.00046	1.66 (1.23–2.25)
padi4_94	167	415	240	822	89	305	252	646	19.86	0.0000084	1.97 (1.44–2.69)
padi4_104[a]	268	355	110	733	313	358	64	735	12.67	0.00051	2.00 (1.41–2.86)[b]
padi4_95	131	386	304	821	64	300	281	645	12.29	0.00046	1.89 (1.35–2.66)
padi4_97	304	390	131	825	283	305	64	652	12.48	0.00041	1.92(1.35–2.70)[b]
padi4_99	225	421	181	827	224	331	100	655	13.72	0.00021	1.82 (1.33–2.44)[b]
padi4_100	225	418	180	823	216	332	98	646	12.00	0.00053	1.75 (1.30–2.38)[b]
padi4_101	222	417	178	817	216	322	95	633	13.62	0.00022	1.82 (1.33–2.50)[b]

Sum of cases > 800; $P < 0.001$.

[a]Control sample number of this SNP was 736. [b]For OR >1, the inverted score is indicated.

exon 3) and padi4_104 (349T→C in exon 4; **Table 1** and **Fig. 2a,b**). Overall, eight SNPs in NT_034376.1 had significant associations with rheumatoid arthritis ($P < 0.001$, **Table 1**), and all these SNPs were in *PADI4*. In the case and control populations, strong linkage disequilibrium extended only within *PADI4* and not to SNPs flanking *PADI4* (**Fig. 1c**). We therefore concluded that the strong association detected with SNPs in *PADI4* originated from *PADI4* itself. Rheumatoid factor status, sex, age at disease onset and *HLA-DRB1* status of affected individuals were not related to *PADI4* genotype distribution (data not shown).

We next undertook full haplotype analysis for 17 SNPs in *PADI4*. Only 4 of 2^{17} possible haplotypes were estimated to have frequency >0.02 in both case and control groups using the expectation-maximization algorithm. Less frequently occurring haplotypes were not shown, owing to concern over the accuracy of low frequency alleles in the expectation-maximization algorithm. The most frequently occurring haplotype, haplotype 1, and the second most frequently occurring haplotype, haplotype 2, comprised more than 85% of total chromosomes both in case and control groups (**Table 2**). Among the SNPs that segregate haplotype 1 and haplotype 2, four were exonic and three of them involved amino acid substitutions: padi4_89, padi4_90, padi4_92 and padi4_104, resulting in G55S, V82A, G112A and L117L, respectively (**Fig. 2c**). Haplotype 1 was more frequently observed in the control group and haplotype 2 in the case group. Haplotype 1 and its transcript and peptide were therefore termed 'non-susceptible', and haplotype 2 and its transcript and peptide 'susceptible'. Compositions of bases and amino acids of transcripts and peptides for susceptible and non-susceptible types are indicated in **Figure 2c**.

Expression of *PADI4* mRNA

To investigate the expression patterns of *PADI4* in tissues, we carried out northern-blot analysis and quantitative real-time RT–PCR. Northern-blot analysis identified two *PADI4* transcripts, one band at 2.6 kb and the other at 4.0 kb (**Fig. 3a**), as described in a previous study[20]. *PADI4* had high levels of expression in bone marrow and peripheral blood leukocytes, low levels of expression in spleen and fetal liver and no expression in other organs (including liver and kidney). *PADI4* was thus highly expressed in the organs of the hematological system.

We also confirmed *PADI4* expression in hematological cell types. Quantitative RT–PCR was done using RNA from $CD4^+$ and $CD8^+$ T cells, $CD19^+$ B cells, $CD14^+$ monocytes, polymorphonuclear leukocytes (PMNs), bone marrow and kidney (as a negative control). *PADI4* was highly expressed in bone marrow, $CD14^+$ monocytes and PMNs but was not expressed in $CD4^+$ and $CD8^+$ T cells or $CD19^+$ B cells (**Fig. 3b**).

Localization of *PADI4* mRNA, protein and citrullinated peptide

To test whether *PADI4* was expressed in rheumatoid arthritis synovial tissues, we carried out *in situ* RT–PCR. We observed *PADI4* mRNA in the lining or sublining layers of synovial tissues from all seven individuals with rheumatoid arthritis that we tested (**Fig. 3c**).

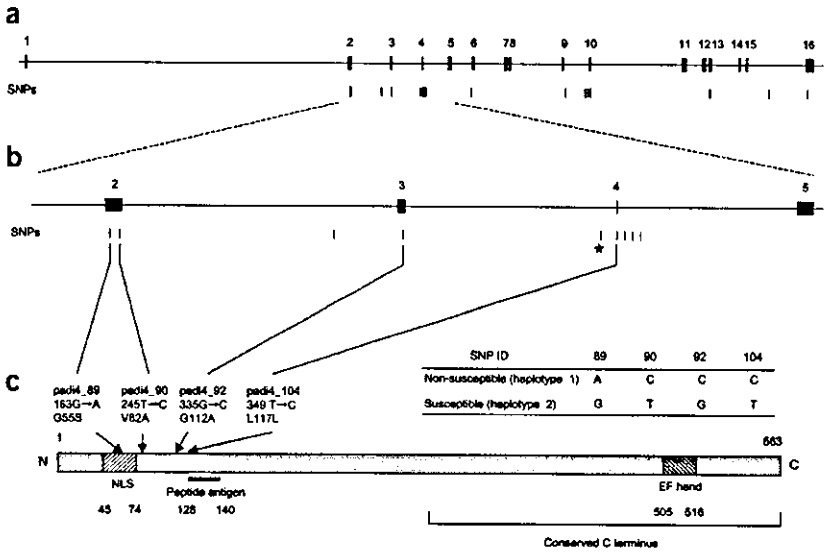

Figure 2 Structure of *PADI4*. (**a**) Exon-intron structure of *PADI4*. SNPs in *PADI4* are indicated below the gene. (**b**) Structure of region including exons 2–5. SNPs in this region are indicated below the gene. The asterisk marks the same SNP that is indicated in **Figure 1b**. (**c**) Protein structure of PADI4. Nucleotide numbering starts from start codons of genes. The bracketed region was used to generate the peptide antibody used in immunohistochemistry.

© 2003 Nature Publishing Group http://www.nature.com/naturegenetics

Table 2 Haplotype structure and frequency in *PADI4*

	Haplotype frequency		SNP ID (as padi4_*x*)															
Haplotype ID	Case	Control	89	90	91	92	93	94	104	95	96	97	98	99	100	101	102	103	105
Haplotype 1	0.52	0.60	A	C	C	C	C	C	C	G	T	T	C	A	T	T	C	T	C
Haplotype 2	0.32	0.25	G	T	T	G	A	T	T	C	C	A	T	G	C	C	C	C	C
Haplotype 3	0.06	0.04	G	T	T	G	A	T	T	C	C	A	T	G	C	C	T	C	C
Haplotype 4	0.06	0.04	G	T	T	G	C	T	C	G	T	T	C	G	C	C	C	T	C

© 2003 Nature Publishing Group http://www.nature.com/naturegenetics

We used sections of synovial tissues for immunohistochemistry with antibodies to PADI4 and to citrulline. In each sample from an individual with rheumatoid arthritis, PADI4 protein was detected in the sublining (**Fig. 3d**). Citrullinated peptide was also detected in the sublining with a similar pattern (**Fig. 3e**). These results indicate that PADI4 protein and citrullinated peptides are localized in rheumatoid arthritis synovia.

Stability of two types of *PADI4* mRNA

To investigate further the association between *PADI4* alleles and rheumatoid arthritis, we tested whether SNPs in exons affect the stability of *PADI4* mRNA. RNAs from the susceptible and non-susceptible alleles (**Fig. 2c**) were transcribed *in vitro* by modified RNase T1 selection assay[21]. Briefly, we mixed RNAs produced by *in vitro* transcription with extracts of HL-60 cells and observed the degradation of RNA by endogenous components of the HL-60 cell. Half-lives for susceptible and non-susceptible *PADI4* mRNA were 11.6 min and 2.1 min, respectively. Susceptible mRNA was therefore significantly more stable than non-susceptible mRNA (after 5 min, $P = 0.038$; after 10 min, $P = 0.017$; **Fig. 4**). Based on this result, mRNA stability seems to depend on haplotype.

Relationship between SNP and antibody to citrullinated filaggrin

Citrullination in proteins is believed to create epitopes recognized by rheumatoid arthritis autoantibodies that not only represent the most specific serologic markers, but also appear early[22], even before clinical onset of rheumatoid arthritis. Citrullinated filaggrin has been used in clinical laboratory tests as a possible candidate for citrullinated autoantigens[23]. We therefore examined the relationship between *PADI4* haplotype and the presence of antibodies to citrullinated filaggrin in sera from individuals with rheumatoid arthritis. Individuals homozygous with respect to the susceptible haplotype were more likely to be positive (87%) for antibody to citrullinated filaggrin than the other two genotypes, for whom the positive fraction rate was 50% (**Table 3**). This tendency was tested using Fisher's exact test and was marginally significant (**Table 4**, $P = 0.038$).

DISCUSSION

A genome-wide association study to identify genes associated with rheumatoid arthritis is in progress in Japan using a high-throughput multiplex PCR-Invader assay[17,18]. Although the project has not yet been completed, one candidate locus has been identified in contig NT_034376.1. Previous sibling-pair linkage studies have also shown that this region is one of the three strongest susceptibility loci for rheumatoid arthritis[5,8]. This locus contains all four identified *PADI* genes, which encode calcium-dependent enzymes that catalyze the conversion of arginine to citrulline in peptides. This activity itself suggested that *PADI* genes may be involved in rheumatoid arthritis, and the antibodies are the most specific rheumatoid arthritis–specific antibodies identified[23–26]. Although several other genes with functional association to rheumatoid arthritis, including that encoding tumor necrosis factor receptor 2 (ref. 27), have been localized to 1p36, *PADI* genes were considered the most relevant for investigation owing to the rheumatoid arthritis specificity of the autoimmune response to citrullinated epitopes.

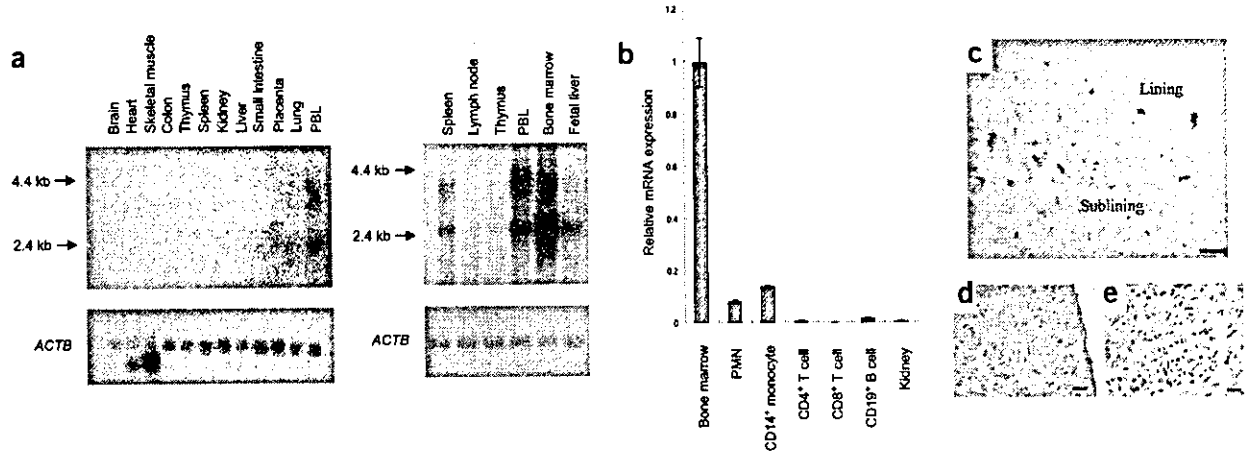

Figure 3 Expression of *PADI4*. (**a**) Expression of *PADI4* mRNA in various normal human tissues. (**b**) Relative expression level of *PADI4* mRNA in normal human tissues and cells. Values represent mean ± s.d. of data from triplicate wells. (**c**) Expression and distribution of *PADI4* mRNA in rheumatoid arthritis synovial tissue as analyzed by *in situ* RT–PCR. *PADI4* transcript (dark blue) was stained in sublining and lining. Immunohistochemistry showing expression patterns of PADI4 (**d**, red stain) and citrullinated peptides (**e**, red stain) in rheumatoid arthritis synovium. No non-rheumatoid arthritis tissue control was used. Scale bars: **c**, 250 μm; **d**, **e**, 100 μm.

We identified eight genes in contig NT_034376.1, including four *PADI* genes (**Fig. 1a**). We evaluated the strength of association with rheumatoid arthritis across the region by linkage disequilibrium mapping of 119 SNPs (**Fig. 1b**). The association in the region was definitive ($P = 0.000008$, OR = 1.97, 95% c.i. = 1.44–2.69) and was considered to originate in *PADI4*, rather than any other *PADI* gene (**Fig. 1c**). We observed a similar pattern of linkage disequilibrium in cases and controls, which is consistent with the association pattern (**Fig. 1c**) and provides additional support for *PADI4* as the origin.

An OR of 1.97 suggests that the genetic contribution of *PADI4* is not as strong as that of the *HLA-DRB* locus (OR = 2.60, 95% c.i. = 1.88–3.60; ref. 28) but is nonetheless considerable. The *HLA-DRB* locus has been estimated to explain less than or close to half of the total genetic contribution to rheumatoid arthritis, with the remainder attributed to multiple non-*HLA* genes[1]. We therefore expect that *PADI4* is one of the primary non-*HLA* genes associated with rheumatoid arthritis. A genotypic risk ratio for *PADI4* is 1.3 (ref. 29), and its population attributable risk is 17.4% (ref. 30), which seems reasonable for a gene associated with a complex genetic trait like rheumatoid arthritis. Furthermore, a locus with this degree of genetic contribution could be detectable in linkage studies, as was the case for microsatellite markers close to *PADI4* in two linkage studies[5,8].

Northern-blot analysis indicated that *PADI4* was highly expressed in bone marrow and peripheral blood leukocytes. Quantitative RT–PCR indicated that *PADI4* mRNA is expressed in PMNs, which include neutrophils and the monocyte lineage, but is not expressed in lymphocytes. Previous reports have shown high *PADI4* expression in neutrophils, eosinophils and monocytes[20,31]. *PADI4* is therefore expressed in hematological tissues and cell types, which are known to be intimately involved in the pathogenesis of rheumatoid arthritis[32,33]. Although the importance of antigen-specific immune processes has been emphasized in the investigation of rheumatoid arthritis, the finding that myeloid leukocytes, rather than lymphocytes, are the predominant cell types in which *PADI4* is expressed indicates that more investigation of the roles of myeloid lineages in rheumatoid arthritis is warranted.

We examined expression of *PADI4* in synovial tissues of seven individuals with rheumatoid arthritis using *in situ* RT–PCR and immunohistochemistry. Both mRNA and protein were expressed in the sublining region, and both PADI4 protein and citrullinated peptide were localized in the sublining region. A previous study reported citrullinated α- and β-fibrin in sublining regions of fibroblast- and macrophage-like mononuclear cells of individuals with rheumatoid arthritis[14]. Peptides in synovial tissues, including fibrins, were proposed to be citrullinated by PADI4 extra- or intracellularly with subsequent secretion, behaving as autoantigens recognized by rheumatoid arthritis–specific antibodies. Lining regions contained *PADI4* mRNA but no protein. The reason for this discrepancy is unclear. Collectively, these data suggest that citrullination by PADI4 occurs in the sublining of synovial tissues and that citrullinated peptides behave as antigens for rheumatoid arthritis–specific autoantibodies. Although the detection of *PADI4* expression in rheumatoid arthritis synovial tissue without comparison to non-rheumatoid arthritis controls does not imply that expression and activity of *PADI4* are specific to rheumatoid arthritis, its presence does support other findings that link rheumatoid arthritis and *PADI4*.

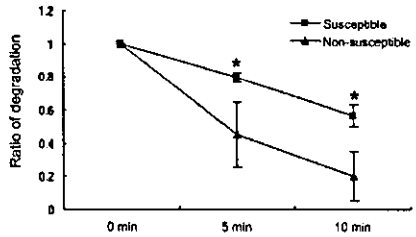

Figure 4 Stability of susceptible and non-susceptible transcripts of *PADI4* mRNA measured as degradation rate. Differences were significant (*$P < 0.05$) after 5 min and 10 min of reaction time. Values represent mean ± s.d. of data from duplicate experiments.

To investigate the relationship between pathogenesis of rheumatoid arthritis and haplotypes comprising the four SNPs in *PADI4* mRNA (**Fig. 2c**), we examined whether these SNPs affect *PADI4* mRNA stability. The mRNA of the susceptible haplotype was more stable than that of the non-susceptible haplotype (**Fig. 4**). In previous studies, SNPs in mRNA or one-base deletions in coding regions have been associated with transcript stability[34,35]. The present result also suggests that SNPs in mRNA contribute to mRNA stability. Susceptible-haplotype mRNA probably accumulates to higher levels than non-susceptible mRNA, resulting in higher levels of PADI4 protein. Stable *PADI4* mRNA may increase PADI4 proteins in synovial tissues, neutrophils and monocytes, increasing production of the citrullinated peptides that serve as autoantigens. Apart from stability of transcripts, evaluation of the effects of substitution of amino acids on the enzyme is important and further investigation should be directed at such analyses. Although SNPs in exons were systematically searched and the effect of coding SNPs analyzed in this report, involvement of other polymorphisms in non-coding regions is possible[35]. Further investigation in intron regions and other regulatory areas is therefore desirable.

The relationship between *PADI4* and rheumatoid arthritis is further supported by the fact that the positive fraction of antibodies to citrullinated peptides was significantly higher in individuals homozygous with respect to the susceptible haplotype than in those of other genotypes ($P = 0.038$, **Table 4**). The present study yielded statistically significant results only in comparing susceptible homozygotes with others and not in comparing non-susceptible homozygotes with others. The absence of a significant difference in the latter comparison might be due to the small number of samples or the mixture of individuals with positive results irrelevant to rheumatoid arthritis–related PADI activity, as should be observed in healthy controls using a test with sensitivity of 75.6%. Previous reports that antibodies to citrullinated peptide are specific to rheumatoid arthritis and are detectable in the early phases of the disease[36] suggest that citrullination by

Table 3 Distribution of individuals of each genotype that were positive for antibody to citrullinated filaggrin

SNP genotype			
Antibody to citrullinated filaggrin	Susceptible homozygotes	Heterozygotes	Non-susceptible homozygotes
Positive	26 (30%)	40 (45%)	22 (25%)
Negative	4 (11%)	20 (57%)	11 (11%)
Positive fraction	0.87	0.50	0.50

© 2003 Nature Publishing Group http://www.nature.com/naturegenetics

Table 4 Association test between genotype and antibody positivity

Comparison pattern	*P* value*
Susceptible homozygotes versus others	0.038
Non-susceptible homozygotes versus others	0.468

**P* value was calculated by Fisher's exact test (two-tailed).

PADI4 should be closely linked to onset of rheumatoid arthritis or might represent a disease-triggering event in itself.

To investigate the precise role of *PADI4* in rheumatoid arthritis, we evaluated the mouse homolog of *PADI4*, *Padi4*, in a collagen-induced arthritis (CIA) mouse model. Expression of *Padi4* was quantified (**Supplementary Fig. 1** online). We induced expression of *Padi4* in inflamed synovial tissues and spleen in mice with CIA. In humans, genotype with respect to *PADI4* was associated with rheumatoid arthritis, presence of PADI4 in affected joints was detected and antibody to citrullinated peptide was detected in sera. In mice, expression of *Padi4* increased with appearance of CIA, but antibody to citrullinated peptide was not detected in sera (data not shown). The primary difference between human rheumatoid arthritis and mouse CIA is that the former is characterized by breakdown of self-tolerance and continuity of destructive arthritis with accompanying autoimmune phenomena to various autoantigens including antibody to citrullinated proteins, whereas the latter shares the inflammatory component related to immune response to collagen type II with rheumatoid arthritis, but specificity of its immunoreaction is higher and breakage of tolerance to citrullinated antigens does not seem to be involved. Given the results of the present study, we consider citrullination by PADI4 or Padi4 as one of the processes in early phase arthritis, and that, in human rheumatoid arthritis, immunological tolerance breaks down somehow with the appearance of autoantibody recognizing citrullinated peptide, followed by the autoimmune disease process characterized for rheumatoid arthritis. In mouse CIA, however, expression of *Padi4* increases with a probable increase in citrullination of self-peptides, but tolerance to citrullinated-antigens does not seem to break. Even with these differences in mechanisms between human rheumatoid arthritis and mouse CIA, further investigation of *PADI4* in human rheumatoid arthritis and *Padi4* in the mouse model seems warranted.

In conclusion, we identified *PADI4* as a susceptibility gene for rheumatoid arthritis using a case-control study with SNPs. The present findings imply that the rheumatoid arthritis susceptibility haplotype in *PADI4* produces a more stable transcript and is associated with higher levels of antibody to citrullinated peptide in sera of individuals with rheumatoid arthritis. Given the polygenic nature of rheumatoid arthritis, this independent susceptibility gene could have a most important role in rheumatoid arthritis pathogenesis by increasing citrullination of proteins in rheumatoid arthritis synovial tissues, leading, in a cytokine-rich milieu, to a break in tolerance to citrullinated peptides processed and presented in the appropriate *HLA* context.

METHODS

Subjects with rheumatoid arthritis and unaffected subjects. We recruited a total of 830 individuals affected with rheumatoid arthritis and 736 unaffected controls for collection of genomic DNA and sera through several medical institutes in Japan. We sampled pathological joint synovial tissues from seven individuals with rheumatoid arthritis who underwent arthroplasty surgery. All rheumatoid arthritis cases met the revised criteria of the American College of Rheumatology for rheumatoid arthritis[37]. The mean age of the 830 case individuals with rheumatoid arthritis was 64.3 y (range, 28–92 y). Most case subjects were female (83.7%), and 75% were positive for rheumatoid factor. Control subjects comprised 736 individuals from the general population, 57.4% females, with mean age of 48.6 y (range, 3–92 y). We obtained informed consent from each subject, with parental authority in the case of minors, as approved by the ethical committee of the SNP Research Center of The Institute of Physical and Chemical Research (RIKEN).

SNPs. We identified four SNPs in exons of *PADI4* and 14 SNPs in *LOC148695* by direct sequencing of DNA from 48 case individuals. We selected the other 101 SNPs, which were located in genes (promoter, exon and intron) in NT_034376.1 (gi: 22043311) from the JST database.

Genotyping. We extracted genomic DNA from peripheral blood leukocytes using standard protocols[17]. We genotyped SNPs using the Invader assay, TaqMan assay or direct sequencing. For Invader assay, we amplified DNA with PCR primers designed to include one or more SNPs, as previously described[18,38]. Third Wave Technologies designed probe sets for each locus. In TaqMan assay, we carried out PCR using TaqMan Universal Master Mix (Applied Biosystems), 8 ng DNA, 1 μM of each primer and 200 nM of probe in 15-μl reactions. Each 96-well plate contained 94 samples of unknown genotype and 2 no-DNA control samples. Thermal cycle conditions were 50 °C for 2 min, 95 °C for 10 min, 50 cycles of 92 °C for 15 s and 58 °C for 1 min. Thermal cycling was done on an ABI PRISM 7700 Sequence Detector Systems (Applied Biosystems). We undertook direct sequencing of PCR products using ABI3700 capillary sequencers (Applied Biosystems) according to standard procedures.

Northern-blot hybridization. We hybridized human multiple tissue northern (MTN) blots (Clontech) with a *PADI4* probe labeled with digoxigenin. We generated digoxigenin-labeled *PADI4* probes using a PCR digoxigenin probe synthesis kit (Roche Diagnostics) according to the manufacturer's instructions, using the primers to generate a 335-bp product. Hybridization and detection were also done according to the manufacturer's instructions. Blots were stripped of probe and re-hybridized with a cDNA probe for *ACTB* (Roche Diagnostics) to assess RNA loading. Primer sequences are available on request.

RNA extraction and cDNA synthesis. We separated PMNs using Mono-Poly resolving solution (Dainippon Pharmaceuticals) and extracted RNA from PMNs using ISOGEN (Nippon Gene). We stored the resulting RNA at –80 °C until use. We quantified RNAs of other normal tissues using Premium total RNA (Clontech). We reverse-transcribed total RNA (1 μg) using a First Strand cDNA synthesis kit (Amersham Pharmacia) according to the manufacturer's instructions.

Quantification of *PADI4* expression by real-time RT–PCR. We carried out real-time PCR on the ABI PRISM 7000 (Applied Biosystems) using QuantiTect SYBR Green PCR (QIAGEN) according to the manufacturer's instructions. Each oligonucleotide primer set was added to a final concentration of 0.3–0.5 μM for *ACTB* (product size, 219 bp) and *PADI4* (product size, 207 bp). We generated a standard curve from data of amplification of *PADI4* primers using a dilution series of bone marrow mRNA as templates and normalized to *ACTB*. Primer sequences are available on request.

***In situ* RT–PCR.** We carried out one-step *in situ* RT–PCR by adding Pro STAR HF (Stratagene), and reactions were done using an Omnislide thermal cycler (Hybaid) as follows: (i) 42 °C for 30 min; (ii) 94 °C for 2 min, 55 °C for 45 s and 68 °C for 2 min; and (iii) 25 cycles at 94 °C for 45 s, 55 °C for 45 s and 68 °C for 2 min. Reactions were maintained at 4 °C after amplification. After PCR, we washed slides twice with Tris-buffered saline for 5 min. Specific primers amplified their specific target sequences, yielding a 335-bp product.

We generated digoxigenin-labeled internal probes by PCR using the PCR digoxigenin probe synthesis kit according to the manufacturer's specification with minor modifications. We added primers to a final concentration of 0.34 μM. We covered slides with pre-hybridization solution at 37 °C for 1 h. After pre-hybridization, we replaced pre-hybridization solution with hybridization

© 2003 Nature Publishing Group http://www.nature.com/naturegenetics

solution containing probe. Probes were denatured at 94 °C for 5 min. We carried out hybridization for 12 h at 37 °C. After washing, we visualized incorporated PCR fragments using a digoxigenin detection kit (Roche Diagnostics).

Controls included several different samples, substituting water for primer in the PCR reaction, omitting reverse transcription in the case of mRNA and omitting probe in hybridization solutions (X.C. *et al.*, manuscript in preparation). Primer sequences are available on request.

Preparation and purification of antiserum against PADI4. We synthesized *PADI4*-derived peptides (Sp-PAD1: PAKKK STGSS TWP-Cys), purified and immunized in rabbits (Kitayama-Labes, Nagano, Japan). We purified antiserum by affinity chromatography on a histidine-tagged PADI4 column (BioGate). We confirmed specificity of purified polyclonal antibody to PADI4 with western blotting using a transient expression system in the HEK293 cell line (data not shown).

Immunohistochemistry. We incubated paraffin sections of synovial tissues at 4 °C for 12 h with rabbit polyclonal antibody to PADI4 or with rabbit antibody to citrulline (Biogenesis), diluted at 1:1,000. We washed and incubated sections at room temperature with Simple Stain MAX-PO (Nichirei) for 30 min and then added Simple Stain AEC (Nichirei). We incubated sections for 5–20 min until the reaction was obviously visible under light microscopy. All sections were counterstained with hematoxylin. In all cases, negative controls omitted the specific antibody and used normal mouse and rabbit antiserum.

Measurement of antibody to citrullinated filaggrin. We measured levels of antibody to citrullinated filaggrin using an ELISA kit (MBL) according to the manufacturer's instructions. Sensitivity was 75.6% and specificity was 83.2% for testing subjects with and without rheumatoid arthritis n clinical settings at a cutoff level of 9 (K. Suzuki *et al.*, manuscript accepted).

***In vitro* RNA stability assay.** We amplified genes encoding two *PADI4* variants by PCR from cDNAs that were synthesized using a first-strand cDNA synthesis kit (Amersham Pharmacia) with bone marrow total RNA (Clontech). We then cloned these genes into the pDONR201 vector (Invitrogen). We also constructed the cDNA into pDEST14 (Invitrogen), which has a T7 promoter, and sequenced both strands of the resulting expression vector. Vectors were digested using *Cla*I, and both types of *PADI4* were expressed using RiboMax Large Scale RNA Production System-T7 (Promega) and purified according to the manufacturer's instructions. To prepare whole-cell extract, we washed HL-60 cells in phosphate-buffered saline and re-suspended them in extraction buffer (0.5% Nonidet P-40; 20 mM HEPES buffer, pH 8.0; 20% glycerol (v/v); 400 mM NaCl, 0.5 mM dithiothreitol; 0.2 mM EDTA and 1% protease inhibitor cocktail (Nacalai)). After incubation on ice for 30 min and microcentrifugation at 4 °C, we transferred supernatants to new tubes and stored them at −80 °C until use.

We mixed and incubated each 5 μg of synthesized RNA and diluted whole-cell extract (1:1,000) at room temperature. The reaction was stopped with the addition of formamide dye, and the samples were then heated at 68 °C. After the reaction, we detected RNA using northern-blot hybridization. We scanned results on a DocuCentre Color 500cp (Fuji-Xerox) and measured signal intensities of full-length RNAs using Adobe Photoshop 6.0.

Statistical analysis. We estimated haplotype frequencies using the expectation-maximization algorithm[39]. We calculated linkage disequilibrium index, Δ (ref. 40), and drew **Figure 1c** with an application created by our group with the assistance of Excel (Microsoft). Associations between phenotypes were estimated by χ^2 test. Antibody to citrullinated filaggrin titer and genotypes were tested using Fisher's exact test on Statistica software (StatSoft), and mRNA stability data and quantitative RT–PCR data were tested using Student's *t*-test.

URLs. The National Center for Biotechnology Information can be found at http://www.ncbi.nlm.nih.gov/. The International RH Mapping Consortium can be found at http://www.ncbi.nlm.nih.gov/genemap99/. The expectation-maximization program can be found at http://linkage.rockefeller.edu/ott/eh.htm.

GenBank accession numbers. *PADI4*, NM_012387; *LOC148695*, XM_088976; *Padi4*, NM_011061.

Note: Supplementary information is available on the Nature Genetics website.

ACKNOWLEDGMENTS

We wish to thank E. Tatsu, K. Kobayashi, M. Mito, N. Iwamoto and the other members of the rheumatoid arthritis team for their advice and technical assistance; H. Kawakami for his expertise in computer programming; and many members of the SNP Research Center for helpful discussions and assistance with various aspects of this study. This work was supported by a grant from the Japanese Millennium Project.

COMPETING INTERESTS STATEMENT

The authors declare that they have no competing financial interests.

Received 25 February; accepted 2 June 2003
Published online 29 June 2003; doi:10.1038/ng1206

1. Seldin, M.F., Amos, C.I., Ward, R. & Gregersen, P.K. The genetics revolution and the assault on rheumatoid arthritis. *Arthritis Rheum.* **42**, 1071–1079 (1999).
2. Gregersen, P.K., Silver, J. & Winchester, R.J. The shared epitope hypothesis. An approach to understanding the molecular genetics of susceptibility to rheumatoid arthritis. *Arthritis Rheum.* **30**, 1205–1213 (1987).
3. Nepom, G.T. Major histocompatibility complex-directed susceptibility to rheumatoid arthritis. *Adv. Immunol.* **68**, 315–332 (1998).
4. Weyand, C.M. & Goronzy, J.J. Association of MHC and rheumatoid arthritis. HLA polymorphisms in phenotypic variants of rheumatoid arthritis. *Arthritis Res.* **2**, 212–216 (2000).
5. Cornelis, F. *et al.* New susceptibility locus for rheumatoid arthritis suggested by a genome-wide linkage study. *Proc. Natl. Acad. Sci. USA* **95**, 10746–10750 (1998).
6. Jawaheer, D. *et al.* A genome-wide screen in multiplex rheumatoid arthritis families suggests genetic overlap with other autoimmune diseases. *Am. J. Hum. Genet.* **68**, 927–936 (2001).
7. MacKay, K. *et al.* Whole-genome linkage analysis of rheumatoid arthritis susceptibility loci in 252 affected sibling pairs in the United Kingdom. *Arthritis Rheum.* **46**, 632–639 (2002).
8. Shiozawa, S. *et al.* Identification of the gene loci that predispose to rheumatoid arthritis. *Int. Immunol.* **10**, 1891–1895 (1998).
9. Schellekens, G.A., de Jong, B.A., van den Hoogen, F.H., van de Putte, L.B. & van Venrooij, W.J. Citrulline is an essential constituent of antigenic determinants recognized by rheumatoid arthritis-specific autoantibodies. *J. Clin. Invest.* **101**, 273–281 (1998).
10. Menard, H.A., Lapointe, E., Rochdi, M.D. & Zhou, Z.J. Insights into rheumatoid arthritis derived from the Sa immune system. *Arthritis Res.* **2**, 429–432 (2000).
11. Schellekens, G.A. *et al.* The diagnostic properties of rheumatoid arthritis antibodies recognizing a cyclic citrullinated peptide. *Arthritis Rheum.* **43**, 155–163 (2000).
12. Nogueira, L. *et al.* Performance of two ELISAs for antifilaggrin autoantibodies, using either affinity purified or deiminated recombinant human filaggrin, in the diagnosis of rheumatoid arthritis. *Ann. Rheum. Dis.* **60**, 882–887 (2001).
13. Goldbach-Mansky, R. *et al.* Rheumatoid arthritis associated autoantibodies in patients with synovitis of recent onset. *Arthritis Res.* **2**, 236–243 (2000).
14. Masson-Bessiere, C. *et al.* The major synovial targets of the rheumatoid arthritis-specific antifilaggrin autoantibodies are deiminated forms of the α- and β-chains of fibrin. *J. Immunol.* **166**, 4177–4184 (2001).
15. Baeten, D. *et al.* Specific presence of intracellular citrullinated proteins in rheumatoid arthritis synovium: relevance to antifilaggrin autoantibodies. *Arthritis Rheum.* **44**, 2255–2262 (2001).
16. Zhou, Z. & Menard, H.A. Autoantigenic posttranslational modifications of proteins: does it apply to rheumatoid arthritis? *Curr. Opin. Rheumatol.* **14**, 250–253 (2002).
17. Ozaki, K. *et al.* Functional SNPs in the lymphotoxin-α gene that are associated with susceptibility to myocardial infarction. *Nat. Genet.* **32**, 650–654 (2002).
18. Ohnishi, Y. *et al.* A high-throughput SNP typing system for genome-wide association studies. *J. Hum. Genet.* **46**, 471–477 (2001).
19. McIntyre, L.M., Martin, E.R., Simonsen, K.L. & Kaplan, N.L. Circumventing multiple testing: a multilocus Monte Carlo approach to testing for association. *Genet. Epidemiol.* **19**, 18–29 (2000).
20. Nakashima, K. *et al.* Molecular characterization of peptidylarginine deiminase in HL-60 cells induced by retinoic acid and 1alpha,25-dihydroxyvitamin D(3). *J. Biol. Chem.* **274**, 27786–27792 (1999).
21. Cuadrado, A. *et al.* HuD binds to three AU-rich sequences in the 3' UTR of neuroserpin mRNA and promotes the accumulation of neuroserpin mRNA and protein. *Nucleic Acids Res.* **30**, 2202–2211 (2002).
22. Vincent, C. *et al.* Detection of antibodies to deiminated recombinant rat filaggrin by enzyme-linked immunosorbent assay: a highly effective test for the diagnosis of rheumatoid arthritis. *Arthritis Rheum.* **46**, 2051–2058 (2002).
23. van Venrooij, W.J. & Pruijn, G.J. Citrullination: a small change for a protein with great consequences for rheumatoid arthritis. *Arthritis Res.* **2**, 249–251 (2000).
24. Vincent, C. *et al.* High diagnostic value in rheumatoid arthritis of antibodies to the stratum corneum of rat oesophagus epithelium, so-called 'antikeratin antibodies'. *Ann. Rheum. Dis.* **48**, 712–722 (1989).
25. Gomes-Daudrix, V. *et al.* Immunoblotting detection of so-called 'antikeratin antibodies': a new assay for the diagnosis of rheumatoid arthritis. *Ann. Rheum. Dis.* **53**, 735–742 (1994).

© 2003 Nature Publishing Group http://www.nature.com/naturegenetics

26. Vincent, C. *et al.* Immunoblotting detection of autoantibodies to human epidermis filaggrin: a new diagnostic test for rheumatoid arthritis. *J. Rheumatol.* **25**, 838–846 (1998).
27. Shibue, T. *et al.* Tumor necrosis factor α 5′-flanking region, tumor necrosis factor receptor II, and HLA-DRB1 polymorphisms in Japanese patients with rheumatoid arthritis. *Arthritis Rheum.* **43**, 753–757 (2000).
28. de Vries, N., Tijssen, H., van Riel, P.L. & van de Putte, L.B. Reshaping the shared epitope hypothesis: HLA-associated risk for rheumatoid arthritis is encoded by amino acid substitutions at positions 67-74 of the HLA-DRB1 molecule. *Arthritis Rheum.* **46**, 921–928 (2002).
29. Risch, N. & Merikangas, K. The future of genetic studies of complex human diseases. *Science* **273**, 1516–1517 (1996).
30. Schildkraut, J.M. Examining complex genetic interactions. in *Approach to Gene Mapping in Complex Human Diseases* (eds. J.L. Haines and M.A. Pericak-Vance) 379–410 (Wiley-Liss, New York, 1998).
31. Asaga, H., Nakashima, K., Senshu, T., Ishigami, A. & Yamada, M. Immunocytochemical localization of peptidylarginine deiminase in human eosinophils and neutrophils. *J. Leukoc. Biol.* **70**, 46–51 (2001).
32. Pillinger, M.H. & Abramson, S.B. The neutrophil in rheumatoid arthritis. *Rheum. Dis. Clin. North Am.* **21**, 691–714 (1995).
33. Hirano, T. Revival of the autoantibody model in rheumatoid arthritis. *Nat. Immunol.* **3**, 342–344 (2002).
34. Zhou, X. *et al.* Association of novel polymorphisms with the expression of SPARC in normal fibroblasts and with susceptibility to scleroderma. *Arthritis Rheum.* **46**, 2990–2999 (2002).
35. Yang, T., McNally, B.A., Ferrone, S., Liu, Y. & Zheng, P. A single nucleotide deletion leads to rapid degradation of TAP-1 mRNA in a melanoma cell line. *J. Biol. Chem.* **278**, 15291–15296 (2003).
36. Jansen, A.L. *et al.* Rheumatoid factor and antibodies to cyclic citrullinated Peptide differentiate rheumatoid arthritis from undifferentiated polyarthritis in patients with early arthritis. *J. Rheumatol.* **29**, 2074–2076 (2002).
37. Arnett, F.C. *et al.* The American Rheumatism Association 1987 revised criteria for the classification of rheumatoid arthritis. *Arthritis Rheum.* **31**, 315–324 (1988).
38. Hirakawa, M. *et al.* JSNP: a database of common gene variations in the Japanese population. *Nucleic Acids Res.* **30**, 158–162 (2002).
39. Ott, J. Counting methods (EM algorithm) in human pedigree analysis: linkage and segregation analysis. *Ann. Hum. Genet.* **40**, 443–454 (1977).
40. Devlin, B. & Risch, N. A comparison of linkage disequilibrium measures for fine-scale mapping. *Genomics* **29**, 311–322 (1995).

© 2003 Nature Publishing Group http://www.nature.com/naturegenetics

ARTHRITIS & RHEUMATISM
Vol. 52, No. 1, January 2005, pp 212–218
DOI 10.1002/art.20741
© 2005, American College of Rheumatology

Significance of Valine/Leucine^{247} Polymorphism of β_2-Glycoprotein I in Antiphospholipid Syndrome

Increased Reactivity of Anti–β_2-Glycoprotein I Autoantibodies to the Valine^{247} β_2-Glycoprotein I Variant

Shinsuke Yasuda,[1] Tatsuya Atsumi,[1] Eiji Matsuura,[2] Keiko Kaihara,[2] Daisuke Yamamoto,[3] Kenji Ichikawa,[1] and Takao Koike[1]

Objective. To clarify the consequences of the valine/leucine polymorphism at position 247 of the β_2-glycoprotein I (β_2GPI) gene in patients with antiphospholipid syndrome (APS), by investigating the correlation between genotypes and the presence of anti-β_2GPI antibody. The reactivity of anti-β_2GPI antibodies was characterized using recombinant Val^{247} and Leu^{247} β_2GPI.

Methods. Sixty-five Japanese patients with APS and/or systemic lupus erythematosus who were positive for antiphospholipid antibodies and 61 controls were analyzed for the presence of the Val/Leu^{247} polymorphism of β_2GPI. Polymorphism assignment was determined by polymerase chain reaction followed by restriction enzyme digestion. Recombinant Val^{247} and Leu^{247} β_2GPI were established to compare the reactivity of anti-β_2GPI antibodies to β_2GPI between these variants. The variants were prepared on polyoxygenated plates or cardiolipin-coated plates, and the reactivity of a series of anti-β_2GPI antibodies (immunized anti-human β_2GPI monoclonal antibodies [Cof-19–21] and autoimmune anti-β_2GPI monoclonal antibodies [EY1C8, EY2C9, and TM1G2]) and IgGs purified from patient sera was investigated.

Results. A positive correlation between the Val^{247} allele and the presence of anti-β_2GPI antibodies was observed in the patient group. Human monoclonal/polyclonal anti-β_2GPI autoantibodies showed higher binding to recombinant Val^{247} β_2GPI than to Leu^{247} β_2GPI, although no difference in the reactivity of the immunized anti-β_2GPI between these variants was observed. Conformational optimization showed that the replacement of Leu^{247} by Val^{247} led to a significant alteration in the tertiary structure of domain V and/or the domain IV–V interaction.

Conclusion. The Val^{247} β_2GPI allele was associated with both a high frequency of anti-β_2GPI antibodies and stronger reactivity with anti-β_2GPI antibodies compared with the Leu^{247} β_2GPI allele, suggesting that the Val^{247} β_2GPI allele may be one of the genetic risk factors for development of APS.

The antiphospholipid syndrome (APS) is characterized by arterial/venous thrombosis and pregnancy morbidity in the presence of antiphospholipid antibodies (aPL) (1–3). Among the targets of aPL, β_2-glycoprotein I (β_2GPI), which bears epitopes for anticardiolipin antibodies (aCL), has been extensively studied (4–6). APS-related aCL do not recognize free β_2GPI, but do recognize β_2GPI when it is complexed with phospholipids or negatively charged surfaces, by exposure of cryptic epitopes (7) or increment of antigen density (8).

The significance of antigen polymorphism in the production of autoantibodies or the development of autoimmune diseases is now being widely discussed. It is speculated that amino acid substitution in antigens can lead to differences in antigenic epitopes of a given protein. In particular, β_2GPI undergoes conformational

[1]Shinsuke Yasuda, MD, PhD, Tatsuya Atsumi, MD, PhD, Kenji Ichikawa, MD, PhD, Takao Koike, MD, PhD: Hokkaido University Graduate School of Medicine, Sapporo, Japan; [2]Eiji Matsuura, PhD, Keiko Kaihara, PhD: Okayama University Graduate School of Medicine, Okayama, Japan; [3]Daisuke Yamamoto, MD, PhD: Osaka Medical College, Takatsuki, Japan.

Address correspondence and reprint requests to Tatsuya Atsumi, MD, PhD, Medicine II, Hokkaido University Graduate School of Medicine, N15 W7, Kita-ku, Sapporo 060-8638, Japan. E-mail: at3tat@med.hokudai.ac.jp.

Submitted for publication May 10, 2004; accepted in revised form September 27, 2004.

alteration upon interaction with phospholipids (9). β_2GPI polymorphism on or near the phospholipid binding site can affect the binding or production of aCL (anti-β_2GPI autoantibodies), the result being altered development of APS. Polymorphism near the antigenic site, or which leads to alteration of the tertiary structure of the whole molecule, may affect the binding of autoantibodies. Five different gene polymorphisms of β_2GPI attributable to a single-nucleotide mutation have been described: 4 are a single amino acid substitution at positions 88, 247, 306, and 316 (10), and the other is a frameshift mutation associated with β_2GPI deficiency found in the Japanese population (11). In particular, the Val/Leu^{247} polymorphism locates in domain V of β_2GPI, between the phospholipid binding site in domain V and the potential epitopes of anti-β_2GPI antibodies in domain IV, as we reported previously (12). Although anti-β_2GPI antibodies are reported to direct to domain I (13) or domain V (14) as well, it should be considered that a certain polymorphism alters the conformation of the molecule, affecting function or antibody binding at a distant site.

We previously reported that, in a group of British Caucasian subjects, the Val^{247} allele was significantly more frequent in primary APS patients with anti-β_2GPI antibodies than in controls or in primary APS patients without anti-β_2GPI antibodies (15), but the importance of the Val^{247} allele in patients with APS is still controversial. In this study, we analyzed the correlation between the β_2GPI Val^{247} allele and anti-β_2GPI antibodies in the Japanese population. We also investigated the reactivity of anti-β_2GPI antibodies to recombinant Val^{247} β_2GPI and Leu^{247} β_2GPI, using a series of monoclonal anti-β_2GPI antibodies and IgGs purified from sera of patients with APS. Finally, to investigate the difference in anti-β_2GPI binding to those variants, we conformationally optimized to domain V and the domain IV–V complex of β_2GPI variants at position 247, referring the crystal structure of β_2GPI.

PATIENTS AND METHODS

Patients and controls. The study group comprised 65 patients (median age 38 years [range 18–74 years]; 57 women and 8 men) who attended the Hokkaido University Hospital, all of whom were positive for aPL (IgG, IgA, or IgM class aCL, and/or lupus anticoagulant). Thirty-four patients had APS (16 had primary APS, and 18 had secondary APS), and 31 patients did not have APS (24 had systemic lupus erythematosus [SLE], and 7 had other rheumatic diseases). Among all subjects, 19 had a history of arterial thrombosis, and 6 had venous thrombosis. Of the 31 patients with a history of pregnancy, 8 experienced pregnancy complications (some patients had more than 1 manifestation of pregnancy morbidity). Anti-β_2GPI antibodies were detected by enzyme-linked immunosorbent assay (ELISA) as β_2GPI-dependent aCL (16). IgG, IgA, or IgM class β_2GPI-dependent aCL were found in 30, 14, and 21 patients, respectively (some patients had >1 isotype), and 34 patients had at least 1 of those isotypes. Lupus anticoagulant, detected by 3 standard methods described previously (17), was found in 51 patients. The diagnoses of APS and SLE, respectively, were based on the preliminary classification criteria for definite APS (18) and the American College of Rheumatology criteria for the classification of SLE (19). Informed consent was obtained from each patient or control subject. The control group comprised 61 healthy individuals with no history of autoimmune, thrombotic, or notable infectious disease.

Determination of β_2GPI gene polymorphism. Genomic DNA was extracted from peripheral blood mononuclear cells (PBMCs) using a standard phenol–chloroform extraction procedure or the DnaQuick kit (Dainippon, Osaka, Japan). Polymorphism assignment was determined by polymerase chain reaction (PCR) followed by allele-specific restriction enzyme digestion (PCR–restriction fragment length polymorphism) using *Rsa* I (Promega, Southampton, UK) as described previously (15).

Purification of patient IgG. Sera from 11 patients positive for IgG class β_2GPI-dependent aCL were collected. The mean (±SD) titer of aCL IgG from these patients was 29.0 ± 21.5 IgG phospholipid (GPL) units (range 12.4 to >98 GPL units). IgG was purified from these sera using a protein G column and the MAbTrap GII IgG purification kit (Pharmacia Biotech, Freiburg, Germany), as recommended by the manufacturer.

Monoclonal anti-β_2GPI antibodies. Two types of anti-β_2GPI monoclonal antibodies were used. Cof-19, Cof-20, and Cof-21 are mouse monoclonal anti-human β_2GPI antibodies obtained from immunized BALB/c mice, directed to domains V, III, and IV of β_2GPI, respectively. These monoclonal antibodies recognize the native structure of human β_2GPI (12).

EY1C8, EY2C9, and TM1G2 are IgM class autoimmune monoclonal antibodies established from patients with APS (20). These antibodies bind to domain IV of β_2GPI, but only after interaction with solid-phase phospholipids or with a polyoxygenated polystyrene surface. EY1C8 and EY2C9 were established from a patient whose genotype of β_2GPI was heterozygous for Val/Leu^{247}. The genotype of the patient with TM1G2 was not determined.

Preparation of recombinant β_2GPI. As previously reported, genes were expressed in *Spodoptera frugiperda* Sf9 insect cells infected with recombinant baculoviruses (12). A full-length complementary DNA of human β_2GPI coding Val^{247} was originally obtained from Hep-G2 cells (21), and the valine residue was replaced by leucine, using the GeneEditor in vitro Site-Directed Mutagenesis System (Promega, Madison, WI). The sequence of the primers for a mutant Val^{247}→Leu (GTA→TTA) is as follows: 5′-GCATCTTGTAAATTACCTGTGAAAAAAG-3′. A DNA sequence of the mutant was verified by analysis using ABI Prism model 310 (PE Applied Biosystems, Foster City, CA).

Binding assays of monoclonal anti-β_2GPI antibodies and purified IgGs to the recombinant β_2GPI (cardiolipin-coated plate). The reactivity of a series of monoclonal anti-β_2GPI antibodies and IgG fractions (purified from the sera of APS patients positive for IgG class anti-β_2GPI) against 2 β_2GPI variants was investigated using an ELISA. ELISAs were performed using a cardiolipin-coated plate as previously reported (16) but with a slight modification. Briefly, the wells of Sumilon Type S microtiter plates (Sumitomo Bakelite, Tokyo, Japan) were filled with 30 μl of 50 μg/ml cardiolipin (Sigma, St. Louis, MO) and dried overnight at 4°C. After blocking with 2% gelatin in phosphate buffered saline (PBS) for 2 hours and washing 3 times with 0.05% PBS–Tween, 50 μl of 10 μg/ml recombinant β_2GPI and controls were distributed and incubated for 30 minutes at room temperature. Wells were filled with 50 μl of serial dilutions of monoclonal antibodies (Cof-19–21, EY1C8 and EY2C9, and TM1G2) or purified patient IgG (100 μg/ml), followed by incubation for 30 minutes at room temperature. After washing 3 times, 50 μl of alkaline phosphatase–conjugated anti-mouse IgG (1:3,000), anti-human IgM (1:1,000), or anti-human IgG (1:6,000) was distributed and incubated for 1 hour at room temperature. The plates were washed 4 times, and 100 μl of 1 mg/ml *p*-nitrophenyl phosphate disodium (Sigma) in 1*M* diethanolamine buffer (pH 9.8) was distributed. Optical density (OD) was read at 405 nm, with reference at 620 nm. One percent fatty acid–free bovine serum albumin (BSA) (A-6003; Sigma)–PBS was used as sample diluent and control.

Binding assays of monoclonal anti-β_2GPI antibodies to recombinant β_2GPI (polyoxygenated plate). Anti-β_2GPI antibody detection assay using polyoxygenated plates was performed as previously reported (22), with minor modifications. Briefly, the wells of polyoxygenated MaxiSorp microtiter plates (Nalge Nunc International, Roskilde, Denmark) were coated with 50 μl of 1 μg/ml recombinant β_2GPI in PBS and incubated overnight at 4°C. After blocking with 3% gelatin–PBS at 37°C for 1 hour and washing 3 times with PBS–Tween, 50 μl of monoclonal antibodies, diluted with 1% BSA–PBS, were distributed and incubated for 1 hour at room temperature. The following steps were taken, in a similar manner.

Conformational optimization of domain V and the domain IV–V complex in human β_2GPI variants at position 247. A conformation of domain V in the valine variant at position 247 was first constructed from the crystal structure of the leucine variant (implemented in Protein Data Bank: 1C1Z) (23). Replacement of leucine by valine at position 247 was performed using the Quanta system (Molecular Simulations, San Diego, CA), and the model was optimized by 500 cycles of energy minimization by the CHARMm program (24), with hydrophilic hydrogen atoms and TIP3 water molecules (25). Molecular dynamics simulation (5 psec) of the model was then performed with 0.002 psec time steps. The cutoff distance for nonbonded interactions was set to 15Å, and the dielectric constant was 1.0. A nonbonded pair list was updated every 10 steps. The most stable structure of each domain in the dynamics iterations was then optimized by 500 cycles of energy minimization. The final structures of domain V consisted of 2,616 atoms, including 603 TIP3 water molecules, and had a total energy of -1.63×10^4 kcal/mole with a root-mean-square force of 0.869 kcal/mole.

Molecular models of a domain IV–V complex (leucine and valine variants at position 247) were further constructed by considering the location of the oligosaccharide attachment site in domain IV, the location of epitopic regions of the Cof-8 and Cof-20 monoclonal antibodies, the junction between domains IV and V, and molecular surface charges of both domains. These models were again optimized by molecular dynamics simulation and by energy minimization as described above. The final structures of the complex in the leucine and valine variants consisted of 3,773 and 3,778 atoms, respectively, including hydrophilic hydrogen atoms and 806 and 808 TIP3 water molecules, respectively, and had total energy of -2.07×104 and -2.03×104 kcal/mole with a root-mean-square force of 0.985 and 0.979 kcal/mole, respectively.

Statistical analysis. Correlations between the allele frequencies and clinical features such as the positiveness of β_2GPI-dependent aCL were expressed as odds ratios (ORs) and 95% confidence intervals (95% CIs). *P* values were determined by chi-square test with Yates' correction. *P* values less than or equal to 0.05 were considered significant.

RESULTS

Val/Leu^{247} polymorphism of β_2GPI and the presence of β_2GPI-dependent aCL. As shown in Table 1, the Leu^{247} allele was dominant in the population of healthy Japanese individuals, compared with Caucasians, which is consistent with a previous report (26). Japanese patients with anti-β_2GPI had a significantly increased frequency of the Val^{247} allele, compared with Japanese patients without anti-β_2GPI ($P = 0.0107$) or Japanese controls ($P = 0.0209$).

The binding of autoimmune anti-β_2GPI to recombinant Val^{247} and Leu^{247} β_2GPI. Representative binding curves using cardiolipin-coated plates and polyoxygenated plates are shown in Figure 1. Regardless of the type of plates, Cof-20 bound equally to valine and leucine variants of β_2GPI (Figures 1a and c), in any concentration of Cof-20. The binding curves of Cof-19 and Cof-21 were similar to that of Cof-20 (results not

Table 1. Frequency of the Val^{247} allele of β_2GPI in patients with APS*

Group	Japanese	British Caucasians
Patients with anti-β_2GPI	23/68 (33.8)†	48/56 (85.7)‡
Patients without anti-β_2GPI	9/62 (14.5)	39/58 (67.2)
Controls	23/122 (18.9)	55/78 (70.5)

* Values are the number (%). β_2GPI - β_2-glycoprotein I; APS - antiphospholipid syndrome.
† $P = 0.0107$ versus patients without anti-β_2GPI (odds ratio [OR] 3.01, 95% confidence interval [95% CI] 1.26–7.16), and $P = 0.0209$ versus controls, by chi-square test (OR 2.15, 95% CI 1.09–4.23).
‡ $P = 0.204$ versus patients without anti-β_2GPI (OR 2.92, 95% CI 1.16–7.39), and $P = 0.0396$ versus controls, by chi-square test (OR 2.51, 95% CI 1.03–6.13).

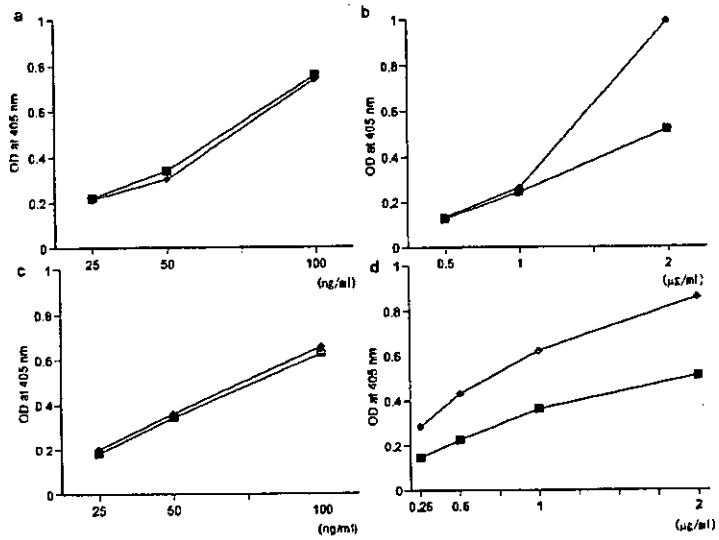

Figure 1. Representative binding curves of monoclonal anti-β_2-glycoprotein I (anti-β_2GPI) antibodies to recombinant valine/leucine^{247} β_2GPI. **a**, Binding curve of Cof-20 using cardiolipin-coated plate. **b**, Binding curve of EY2C9 using cardiolipin-coated plate. **c**, Binding curve of Cof-20 using polyoxygenated plate. **d**, Binding curve of EY2C9 using polyoxygenated plate. Binding to Val^{247} β_2GPI and Leu^{247} β_2GPI are indicated with diamonds and squares, respectively. OD = optical density.

shown). In contrast, EY2C9 showed stronger binding to Val^{247} β_2GPI than to Leu^{247} β_2GPI (Figures 1b and d). EY1C8 and TM1G2 also showed stronger binding to Val^{247} β_2GPI. Figure 2a shows the binding of the monoclonal antibodies, on cardiolipin-coated plates, in the following concentrations: for Cof-19–21, 100 ng/ml;

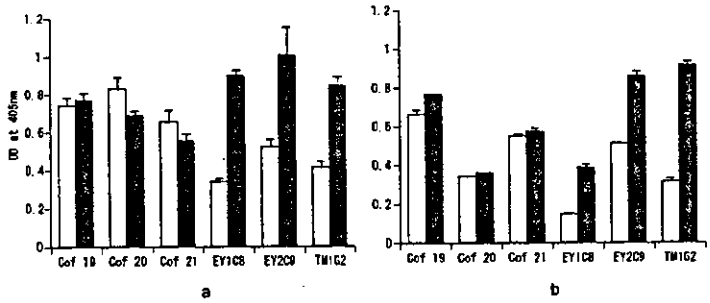

Figure 2. Reactivity of anti-β_2-glycoprotein I (anti-β_2GPI) antibodies to β_2GPI variants. **a**, The binding of monoclonal anti-β_2GPI antibodies to the recombinant valine/leucine^{247} β_2GPI was investigated using enzyme-linked immunosorbent assay (ELISA) on cardiolipin-coated plates. Concentrations of antigens and antibodies were as follows: for recombinant β_2GPI, 10 μg/ml; for Cof-19–21, 100 ng/ml; for EY1C8 and EY2C9, 2 μg/ml; for TM1G2, 5 μg/ml. **b**, The binding of monoclonal anti-β_2GPI antibodies to the recombinant Val/Leu^{247} β_2GPI was investigated using ELISA on polyoxygenated plates. Concentrations of antigens and antibodies were as follows: for recombinant β_2GPI, 1 μg/ml; for Cof-19–21, 50 ng/ml; for EY1C8 and EY2C9, 2 μg/ml; for TM1G2, 5 μg/ml. Results were presented as the optical density (OD) at 405 nm. Open columns indicate binding activity to Leu^{247} β_2GPI, and solid columns indicate binding activity to Val^{247} β_2GPI. Bars show the mean and SD.

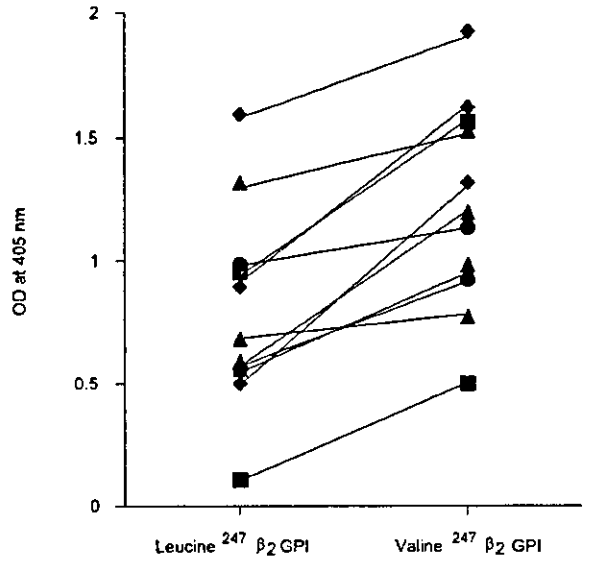

Figure 3. Reactivity of purified IgG from patients (100 μg/ml) to recombinant Val/Leu^{247} β_2-glycoprotein I (β_2GPI) (10 μg/ml), presented as the optical density (OD) at 405 nm. Squares, circles, and triangles indicate patients homozygous for the Leu^{247} allele, homozygous for the Val^{247} allele, and heterozygous for the Val/Leu^{247} allele, respectively. Diamonds indicate patients whose genotypes were not available.

for EY1C8 and EY2C9, 1 μg/ml; and for TM1G2, 2.5μg/ml. In contrast with the close reactivity of Cof-19, Cof-20, and Cof-21 between Val^{247} β_2GPI and Leu^{247} β_2GPI, autoimmune monoclonal antibodies (EY1C8, EY2C9, and TM1G2) showed higher binding to Val^{247} β_2GPI than to Leu^{247} β_2GPI. The autoimmune monoclonal antibodies also showed a higher binding to Val^{247} β_2GPI directly coated on polyoxygenated plates (Figure 2b). IgG in sera collected from 11 patients (100 μg/ml) also showed higher binding to Val^{247} β_2GPI than to Leu^{247} β_2GPI on cardiolipin-coated plates, regardless of the patients' genotypes (Figure 3).

Conformational alteration by leucine replacement by valine at position 247. Each domain V conformation in 2 variants at position 247 is shown in Figure 4a. The root-mean-square deviations for matching backbone atoms and equivalent atoms in the leucine and valine variants were 0.76 and 1.11 Å, respectively. The largest shift was observed at Val^{303}, one of the residues located on the backbone neighboring position 247. The shift seemed to be caused by weak flexibility of side chains consisting of Val^{247}, Pro^{248}, and Val^{249} and the electrostatic interactions between Lys^{250}, Lys^{251}, Glu^{307}, and Lys^{308}.

The molecular models of the IV–V complex in leucine and valine variants are shown in Figure 4b. The root-mean-square deviations for matching these backbone atoms and equivalent atoms were 1.72 and 2.03 Å, respectively. Electrostatic interactions and hydrogen bonds between Asp^{193} and Lys^{246}/Lys^{250}, Asp^{222} and Lys^{305}, and Glu^{228} and Lys^{308} appeared in the IV–V complex, but the interaction between Glu^{228} and Lys^{308} was disrupted by the leucine replacement by valine, because direction of the Lys^{308} side chain was significantly changed in the complex. As a result, Trp^{235} of domain IV, located on the contact surface with domain V, was slightly shifted.

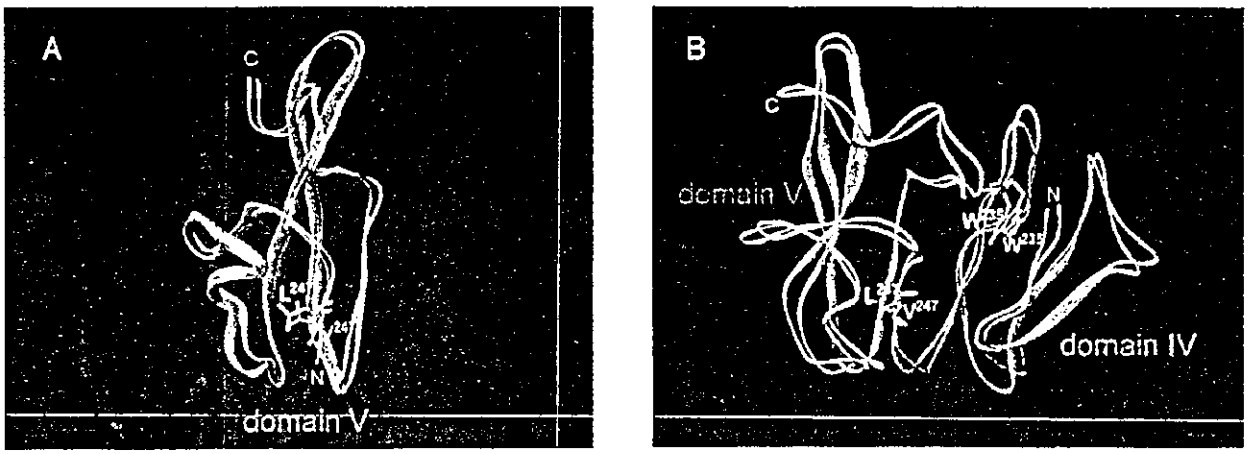

Figure 4. Conformational alterations in domain V (A) and in the domain IV–V complex (B), replacing leucine by valine at position 247. Structure of the valine (light blue) and leucine (white) variants was shown by a ribbon representation with the secondary structure.

DISCUSSION

This study shows the positive correlation between the Val^{247} β_2GPI allele and anti-β_2GPI antibody production in a Japanese population, confirming the correlation observed in a British Caucasian population in our previous report (15). A positive correlation between the Val^{247} allele and the presence of anti-β_2GPI antibodies was also reported in Asian American (26) and Mexican patients (27). However, this correlation was not observed in other American populations (26) or in patients with thrombosis or pregnancy complications in the UK (28). This discrepancy may be the result of the difference in the frequency of the Val^{247} allele among races, or the difference in the background of investigated patients. Another possibility is that the relationship between the Val^{247} allele and thrombosis in Caucasians may be controversial due to underpowered studies or to differences in the procedure used to detect anti-β_2GPI antibodies. Methods for the detection of anti-β_2GPI antibodies differ among laboratories. For example, cardiolipin-coated plates or oxygenated plates are used in some methods, whereas unoxygenated plates are used in others. In addition, bovine β_2GPI is used instead of human β_2GPI in some assays. The antibodies used for standardization also differ, although monoclonal antibodies such as EY2C9 and HCAL (29) have been proposed as international standards of calibration materials.

β_2GPI is a major target antigen for aCL, and, according to our previous investigation, B cell epitopes reside in domain IV and are considered to be cryptic and to appear only when β_2GPI interacts with negatively charged surfaces such as cardiolipin, phosphatidylserine, or polyoxygenated polystyrene surface (7), although other studies indicate that the B cell epitopes are located on domain I (13) or domain V (14). According to another interpretation for the specificity of aCL, increment of the local antigen density on the negatively charged surface also contributes to anti-β_2GPI detection in ELISA (8,30). Studies on the crystal structure of human β_2GPI revealed that the lysine-rich site and an extended C-terminal loop region on domain V are crucial for phospholipid binding. Position 247 is located at the N-terminal side of domain V, and, around this position, Lys^{242}, Ala^{243}, and Ser^{244} were suggested to play a role in the interaction between domains IV and V (9,23,31).

Although the Val/Leu^{247} polymorphism may not be very critical for the autoantibody binding, the amino acid substitution at this point was revealed to affect the affinity of monoclonal aCL established from patients with APS and that of purified IgG from patients positive for β_2GPI-dependent aCL. We conformationally optimized to domain V and the domain IV–V complex of β_2GPI variants at position 247, referring the crystal structure of β_2GPI. IgG aCL was screened using the standardized aCL ELISA, in which both the Leu^{247} and the Val^{247} allele of β_2GPI are contained as antigen. Although biochemical characteristics and structure are similar between valine and leucine, the replacement of Leu^{247} by Val^{247} leads to a significant alteration in the tertiary structure of domain V and/or the domain IV–V interaction (Figure 4). It is likely that the structural alteration affects the affinity between anti-β_2GPI autoantibodies and the epitope(s) present on its molecule. One explanation for this phenomenon is that this β_2GPI polymorphism affects the electrostatic interaction between domain IV and domain V or the protein–protein interaction, resulting in differences in the accessibility of the recognition site by the autoantibodies, or the local density of β_2GPI.

Another possible explanation of the correlation between the Val/Leu^{247} polymorphism of β_2GPI and anti-β_2GPI antibodies is T cell reactivity. Ito et al (32) investigated T cell epitopes of patients with anti-β_2GPI autoantibodies by stimulating patients' PBMCs with a peptide library that covers the β_2GPI sequence. Four of 7 established CD4+ T cell clones reacted to peptide fragments that include amino acid position 244–264, then position 247 is included among the candidate epitopes. Arai et al (33) found preferred recognition of peptide position 276–290 by T cell clones from patients with APS. They also found high reactivity to peptide 247–261 in one patient. We speculate that a small alteration in the conformation arising from the valine/leucine substitution at position 247 may affect the susceptibility to generate autoreactive T cell clones in patients with APS.

Our results in this study indicate that the Val/Leu^{247} polymorphism affects the antigenicity of β_2GPI for anti-β_2GPI autoantibodies, and that the Val^{247} allele can be a risk factor for having autoantibodies against this molecule. Therefore, the Val/Leu^{247} variation of β_2GPI may be crucial for autoimmune reactivity against β_2GPI. We further show the significance of the Val/Leu^{247} polymorphism of β_2GPI in the strength of the binding between β_2GPI and anti-β_2GPI autoantibodies. The significance of antigen polymorphisms in the production of autoantibodies or in the development of autoimmune diseases is not well understood. To our knowledge, this report is the first to present a genetic polymorphism of

autoantigen directly affecting its interaction with autoantibodies.

REFERENCES

1. Hughes GR. The antiphospholipid syndrome: ten years on. Lancet 1993;342:341–4.
2. Hughes GR. Harris EN. Gharavi AE. The anticardiolipin syndrome. J Rheumatol 1986;13:486–9.
3. Harris EN. Gharavi AE. Hughes GR. Anti-phospholipid antibodies. Clin Rheum Dis 1985;11:591–609.
4. Galli M. Comfurius P. Maassen C. Hemker HC. de Baets MH. van Breda-Vriesman PJ. et al. Anticardiolipin antibodies (ACA) directed not to cardiolipin but to a plasma protein cofactor. Lancet 1990;335:1544–7.
5. McNeil HP. Simpson RJ. Chesterman CN. Krilis SA. Anti-phospholipid antibodies are directed against a complex antigen that includes a lipid-binding inhibitor of coagulation: β_2-glycoprotein I (apolipoprotein H). Proc Natl Acad Sci U S A 1990;87:4120–4.
6. Matsuura E. Igarashi Y. Fujimoto M. Ichikawa K. Koike T. Anticardiolipin cofactor(s) and differential diagnosis of autoimmune disease. Lancet 1990;336:177–8.
7. Matsuura E. Igarashi Y. Yasuda T. Triplett DA. Koike T. Anticardiolipin antibodies recognize β_2-glycoprotein I structure altered by interacting with an oxygen modified solid phase surface. J Exp Med 1994;179:457–62.
8. Roubey RA. Eisenberg RA. Harper MF. Winfield JB. "Anticardiolipin" autoantibodies recognize β_2-glycoprotein I in the absence of phospholipid: importance of Ag density and bivalent binding. J Immunol 1995;154:954–60.
9. Schwarzenbacher R. Zeth K. Diederichs K. Gries A. Kostner GM. Laggner P. et al. Crystal structure of human β_2-glycoprotein I: implications for phospholipid binding and the antiphospholipid syndrome. EMBO J 1999;18:6228–39.
10. Sanghera DK. Kristensen T. Hamman RF. Kamboh MI. Molecular basis of the apolipoprotein H (β_2-glycoprotein I) protein polymorphism. Hum Genet 1997;100:57–62.
11. Yasuda S. Tsutsumi A. Chiba H. Yanai H. Miyoshi Y. Takeuchi R. et al. β_2-glycoprotein I deficiency: prevalence, genetic background and effects on plasma lipoprotein metabolism and hemostasis. Atherosclerosis 2000;152:337–46.
12. Igarashi M. Matsuura E. Igarashi Y. Nagae H. Ichikawa K. Triplett DA. et al. Human β_2-glycoprotein I as an anticardiolipin cofactor determined using mutants expressed by a baculovirus system. Blood 1996;87:3262–70.
13. Iverson GM. Victoria EJ. Marquis DM. Anti-β_2 glycoprotein I (β_2GPI) autoantibodies recognize an epitope on the first domain of β_2GPI. Proc Natl Acad Sci U S A 1998;95:15542–6.
14. Wang MX. Kandiah DA. Ichikawa K. Khamashta M. Hughes G. Koike T. et al. Epitope specificity of monoclonal anti-β_2-glycoprotein I antibodies derived from patients with the antiphospholipid syndrome. J Immunol 1995;155:1629–36.
15. Atsumi T. Tsutsumi A. Amengual O. Khamashta MA. Hughes GR. Miyoshi Y. et al. Correlation between β_2-glycoprotein I valine/leucine^{247} polymorphism and anti-β_2-glycoprotein I antibodies in patients with primary antiphospholipid syndrome. Rheumatology (Oxford) 1999;38:721–3.
16. Matsuura E. Igarashi Y. Fujimoto M. Ichikawa K. Suzuki T. Sumida T. et al. Heterogeneity of anticardiolipin antibodies defined by the anticardiolipin cofactor. J Immunol 1992;148:3885–91.
17. Atsumi T. Ieko M. Bertolaccini ML. Ichikawa K. Tsutsumi A. Matsuura E. et al. Association of autoantibodies against the phosphatidylserine-prothrombin complex with manifestations of the antiphospholipid syndrome and with the presence of lupus anticoagulant. Arthritis Rheum 2000;43:1982–93.
18. Wilson WA. Gharavi AE. Koike T. Lockshin MD. Branch DW. Piette JC. et al. International consensus statement on preliminary classification criteria for definite antiphospholipid syndrome: report of an international workshop. Arthritis Rheum 1999;42:1309–11.
19. Tan EM. Cohen AS. Fries JF. Masi AT. McShane DJ. Rothfield NF. et al. The 1982 revised criteria for the classification of systemic lupus erythematosus. Arthritis Rheum 1982;25:1271–7.
20. Ichikawa K. Khamashta MA. Koike T. Matsuura E. Hughes GR. β_2-glycoprotein I reactivity of monoclonal anticardiolipin antibodies from patients with antiphospholipid syndrome. Arthritis Rheum 1994;37:1453–61.
21. Matsuura E. Igarashi M. Igarashi Y. Nagae H. Ichikawa K. Yasuda T. et al. Molecular definition of human β_2-glycoprotein I (β_2-GPI) by cDNA cloning and inter-species differences of β_2-GPI in alternation of anticardiolipin binding. Int Immunol 1991;3:1217–21.
22. Matsuura E. Igarashi Y. Yasuda T. Triplett DA. Koike T. Anticardiolipin antibodies recognize β_2-glycoprotein I structure altered by interacting with an oxygen modified solid phase surface. J Exp Med 1994;179:457–62.
23. Bouma B. de Groot PG. van den Elsen JM. Ravelli RB. Schouten A. Simmelink MJ. et al. Adhesion mechanism of human β_2-glycoprotein I to phospholipids based on its crystal structure. EMBO J 1999;18:5166–74.
24. Brooks BR. Bruccoleri RE. Olafson BD. States DJ. CHARMm: a program for macromolecular energy, minimization: and dynamics calculations. J Comput Chem 1983;4:187–217.
25. Carlson W. Karplus M. Haber E. Construction of a model for the three-dimensional structure of human renal renin. Hypertension 1985;7:13–26.
26. Hirose N. Williams R. Alberts AR. Furie RA. Chartash EK. Jain RI. et al. A role for the polymorphism at position 247 of the β_2-glycoprotein I gene in the generation of anti-β_2-glycoprotein I antibodies in the antiphospholipid syndrome. Arthritis Rheum 1999;42:1655–61.
27. Prieto GA. Cabral AR. Zapata-Zuñiga M. Simón AI. Villa AR. Alarcon-Segovia D. et al. Valine/valine genotype at position 247 of the β_2-glycoprotein I gene in Mexican patients with primary antiphospholipid syndrome: association with anti-β_2-glycoprotein I antibodies. Arthritis Rheum 2003;48:471–4.
28. Camilleri RS. Mackie IJ. Humphries SE. Machin SJ. Cohen H. Lack of association of β_2-glycoprotein I polymorphisms Val247Leu and Trp316Ser with antiphospholipid antibodies in patients with thrombosis and pregnancy complications. Br J Haematol 2003;120:1066–72.
29. Ichikawa K. Tsutsumi A. Atsumi T. Matsuura E. Kobayashi S. Hughes GR. et al. A chimeric antibody with the human γ1 constant region as a putative standard for assays to detect IgG β_2-glycoprotein I-dependent anticardiolipin and anti-β_2-glycoprotein I antibodies. Arthritis Rheum 1999;42:2461–70.
30. Tincani A. Spatola L. Prati E. Allegri F. Ferremi P. Cattaneo R. et al. The anti-β_2-glycoprotein I activity in human anti-phospholipid syndrome sera is due to monoreactive low-affinity autoantibodies directed to epitopes located on native β_2-glycoprotein I and preserved during species' evolution. J Immunol 1996;157:5732–8.
31. Saxena A. Gries A. Schwarzenbacher R. Kostner GM. Laggner P. Prassl R. Crystallization and preliminary x-ray crystallographic studies on apolipoprotein H (β_2-glycoprotein-I) from human plasma. Acta Crystallogr D Biol Crystallogr 1998;54:1450–2.
32. Ito H. Matsushita S. Tokano Y. Nishimura H. Tanaka Y. Fujisao S. et al. Analysis of T cell responses to the β_2-glycoprotein I-derived peptide library in patients with anti-β_2-glycoprotein I antibody-associated autoimmunity. Hum Immunol 2000;61:366–77.
33. Arai T. Yoshida K. Kaburagi J. Inoko H. Ikeda Y. Kawakami Y. et al. Autoreactive CD4+ T-cell clones to β_2-glycoprotein I in patients with antiphospholipid syndrome: preferential recognition of the major phospholipid-binding site. Blood 2001;98:1889–96.